Polyoxometalates

DOI: 10.1002/anie.200902483

Polyoxometalates: Building Blocks for Functional Nanoscale Systems

*De-Liang Long, Ryo Tsunashima, and Leroy Cronin**

Keywords:
cluster compounds · metal oxides · self organization · nanoscience · polyoxometalates

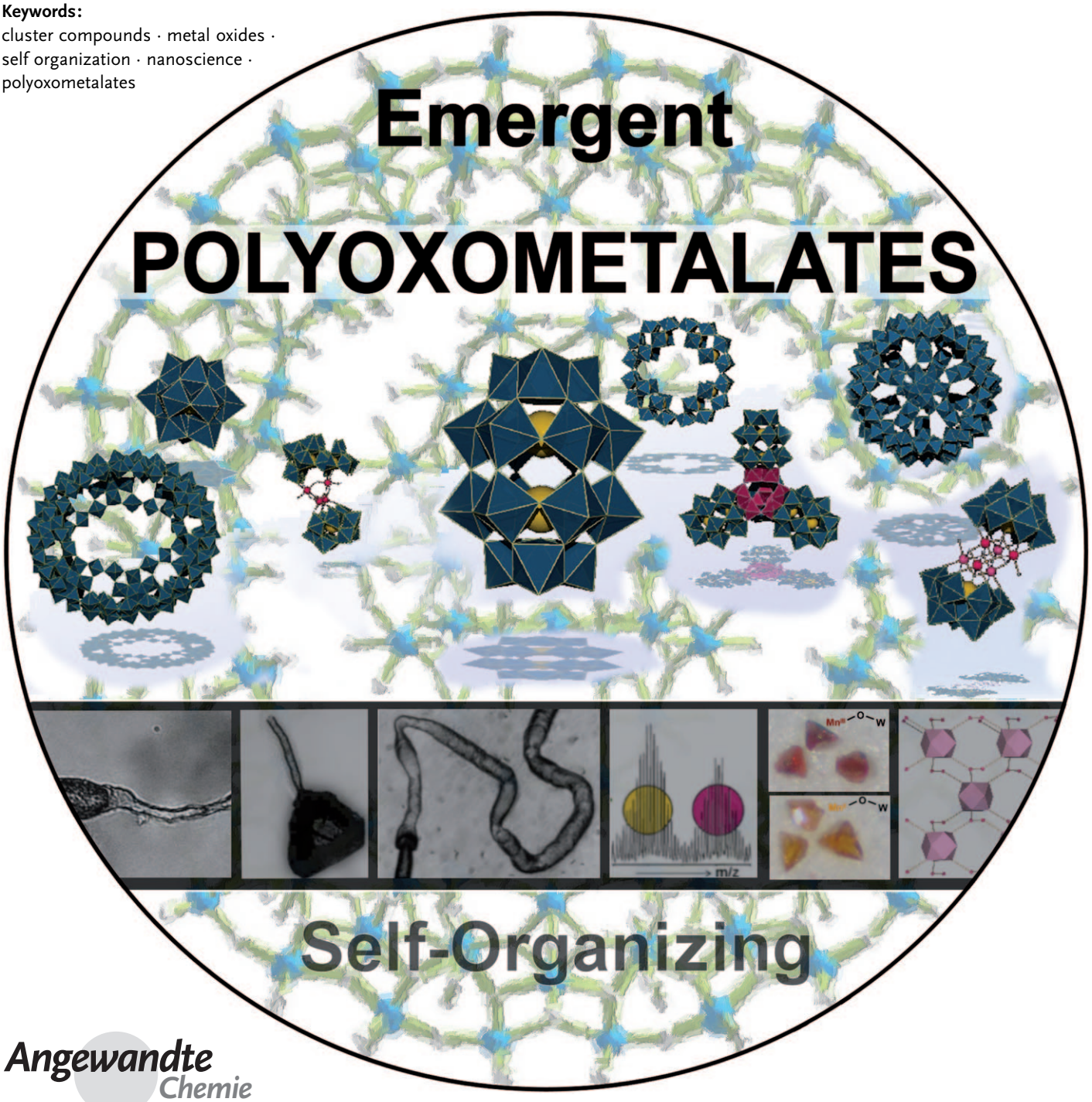

© 2010 Wiley-VCH Verlag GmbH & Co. KGaA, Weinheim

Polyoxometalates (POMs) are a subset of metal oxides that represent a diverse range of molecular clusters with an almost unmatched range of physical properties and the ability to form dynamic structures that can range in size from the nano- to the micrometer scale. Herein we present the very latest developments from synthesis to structure and function of POMs. We discuss the possibilities of creating highly sophisticated functional hierarchical systems with multiple, interdependent, functionalities along with a critical analysis that allows the non-specialist to learn the salient features. We propose and present a "periodic table of polyoxometalate building blocks". We also highlight some of the current issues and challenges that need to be addressed to work towards the design of functional systems based upon POM building blocks and look ahead to possible emerging application areas.

From the Contents

1. The Growth in Polyoxometalate Chemistry

Polyoxometalate (POM) clusters have an unmatched range of physical and chemical properties, acting as a set of transferable building blocks that can be reliably utilized in the formation of new materials. These key features are being exploited rapidly today after a rise in popularity of POMs, which started in the early 1990s as a result of a Review by Pope and Müller[1] in 1991 that foresaw the present explosion. The vast growth was also well-documented in 1998, when a special thematic issue in *Chemical Reviews* organized by Hill presented the history, developments, and application of the many areas covered by POM chemistry.[2]

Today, POM chemistry is a key emerging area that promises to allow the development of sophisticated designer molecule-based materials and devices that exploit developments in instrumentation, nanoscale science, and material fabrication methods. However, despite all the promise, the relentless increase in the number of structures and derivatives mean that it can be difficult to distinguish between the different cluster types and subtypes. The reason for the explosion in the number of structurally characterized POM compounds is due to developments in instrumentation and novel synthetic approaches. In terms of technique development, fast and routine single crystal data collection has allowed the area to accelerate to the point that the bottle neck has moved to structure refinement or to crystallization of new compounds rather than the time taken for data collection and initial structure solution. There are over 500 papers (not including patents) published each year that involve at least some aspect of POM chemistry, and this number is rapidly increasing (Figure 1). In the last few years, a number of Reviews have appeared that address different aspects of POM science, including new structures, biomedical applications, catalysis, theoretical calculations, and perspectives for new materials.[3,4] Herein, we will focus on very recent developments that have enabled new synthetic routes, analysis, self assembly to nanostructures, design of functional systems. Of course, the inspiration for much of these concepts comes from early pioneering work,[1,2] which demonstrates the fundamental idea that polyoxometalate-based nanosystems with well-defined functionality could be possible.[3]

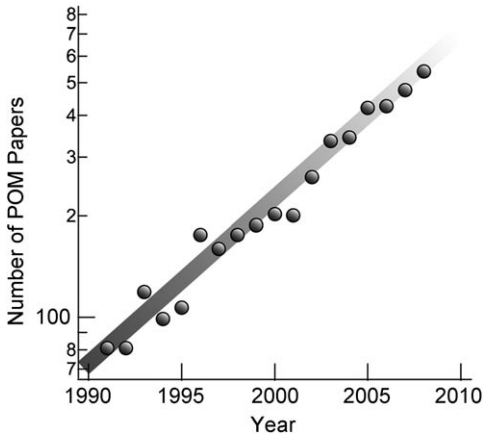

Figure 1. The number of publications that involve the study of polyoxometalates plotted against the year. The *y* axis is plotted on a logarithmic scale showing a linear trend.

This review aims to be not only a snapshot of the recent developments made during the past couple of years in terms of design, architecture, and application, but also to be employed as a guide to understand the many different cluster types and subtypes, and in particular to understand the structural formulae. We place a special emphasis on systems that show multifunctionality and on how the cluster templates, resulting building blocks, sub-structures, and overall

[*] Dr. D.-L. Long, Dr. R. Tsunashima, Prof. L. Cronin
WestCHEM, Department of Chemistry
The University of Glasgow
University Avenue, Glasgow G12 8QQ, Scotland (UK)
Fax: (+44) 141-330-4888
E-mail: L.Cronin@chem.gla.ac.uk
Homepage: http://www.croninlab.com

© 2010 Wiley-VCH Verlag GmbH & Co. KGaA, Weinheim

cluster architecture need to be manipulated at every level to produce a hierarchical functional molecular-cluster-based material. We will attempt to link together new areas and suggest some possible new avenues. In particular, we attempt to try and highlight POM systems that show or have potential to present a hierarchy of properties that may be successively "designed-in" to make highly sophisticated materials.

2. Classification and Design Principles

There are many thousands of compounds which fall into the polyoxometalate category, and they come in a vast range of shapes and sizes with a seemingly endless number of structure types; therefore, understanding the relationships between the different cluster types can be bewildering. However it is possible to broadly classify polyoxometalates, which can help in the conceptualization and understanding of the many structural types. This classification of course has limitations and exceptions, but we will briefly explain a general approach with the aim of helping the reader make the link between different types of building blocks, structures, and physical properties. In general, the class of compounds known as polyoxometalates are based upon metal oxide building blocks with a general formula $\{MO_x\}_n$, where M = Mo, W, V, and sometimes Nb and $x = 4$–7.[1] Overall, POM clusters are normally anionic and thus can be complexed with additional cations as linkers, which can include heteroatom templates, and they can also form lacunary structures, whereby some of the cage atoms are removed to create vacancies that can be filled by linker atoms. Figure 2 presents a classification of the polyoxometalate formulae that are currently known, and also shows how the structures relate to each other in a "polyoxometalate periodic table". This table encompasses the nuclearity, type, and the broad range of structures presently known. Figure 3 shows how the structures of polyoxometalates can be broken down into three broad subsets:

1) *Heteropolyanions* are metal oxide clusters that include heteroanions such as SO_4^{2-} and PO_4^{3-}. These are by far the most explored subset of POM clusters; much of this research has examined the catalytic properties of POMs, with great emphasis on the archetypal Keggin $[XM_{12}O_{40}]^{n-}$ and Wells–Dawson $[X_2M_{18}O_{62}]^{n-}$ anions (where M = W or Mo; X is a tetrahedral template). Tungsten-based POMs are robust, and this fact has been exploited to develop tungsten-based Keggin and Dawson anions with vacancies (most commonly with one, two, or three vacancies) that can be linked using electrophiles to larger aggregates in a predictable manner. The development of lacunary polyoxometalates based upon Keggin $\{M_{12-n}\}$ and Dawson $\{M_{18-n}\}$, tungsten-based polyoxometalates is a large research area and will not be explicitly covered here in detail; however, some guiding principles will be discussed to allow the critical evaluation of the literature.[9]
2) *Isopolyanions* are composed of a metal oxide framework, but without the internal heteroatom/heteroanion. As a result, they are often much more unstable than their heteropolyanion counterparts.[10] However they also have interesting physical properties, such as high charges and strongly basic oxygen surfaces, which means they are attractive units for use as building blocks.[11]
3) *Molybdenum blue and molybdenum brown reduced POM clusters* are related to molybdenum blue species, which was first reported by Scheele in 1783. Their composition was largely unknown until Müller et al. reported the synthesis and structural characterization in 1995 of a very-high-nuclearity cluster $\{Mo_{154}\}$, which has a ring topology, that crystallized from a solution of molybdenum blue.[12] Changing the pH and increasing the amount of reducing agent along with incorporation of acetate ligands facilitates the formation of a $\{Mo_{132}\}$ spherical ball-like cluster.[13] This class of highly reduced POM clusters is one of the most exciting developments in POM chemistry with many potential spin off applications in nanoscience, and it will be discussed in Sections 3 and 6.

2.1. Synthetic Strategies

Polyoxometalate clusters occupy a vast parameter space between the mononuclear metalate species and the bulk oxide. Incorporation of heteroatom templates, heterometalic centers, lacunary building blocks, different protonation states, cations, and ligands all dramatically affect the overall architecture. The architectural design principles are almost

De-Liang Long received his B.Sc. and M.Sc. degrees in chemistry from Wuhan University (China) and completed his Ph.D. under the direction of Professor Xin-Quan Xin at Nanjing University in 1996. After a postdoctoral appointment at Fujian Institute of Research on the Structure of Matter, Chinese Academy of Sciences, in 1999, he held the Royal Society KC Wong Fellowship working with Professor Martin Schröder at the University of Nottingham. He is currently a Senior Research Fellow (Reader) in Professor Lee Cronin's group. His interests are in inorganic synthesis, coordination chemistry, crystallography, and cluster-based materials.

Ryo Tsunashima completed his Ph.D. under the direction of Professor Takayoshi Nakamura at Hokkaido University (Japan) in 2007. Following a postdoctoral appointment at the Research Institute for Electronic Science, Hokkaido University, he is currently a Research Associate with Professor Lee Cronin at the University of Glasgow. His interests are in polyoxometalate synthesis, the development of POM-based molecular nanosystems, supramolecular chemistry, and molecularly thin films.

 © 2010 Wiley-VCH Verlag GmbH & Co. KGaA, Weinheim

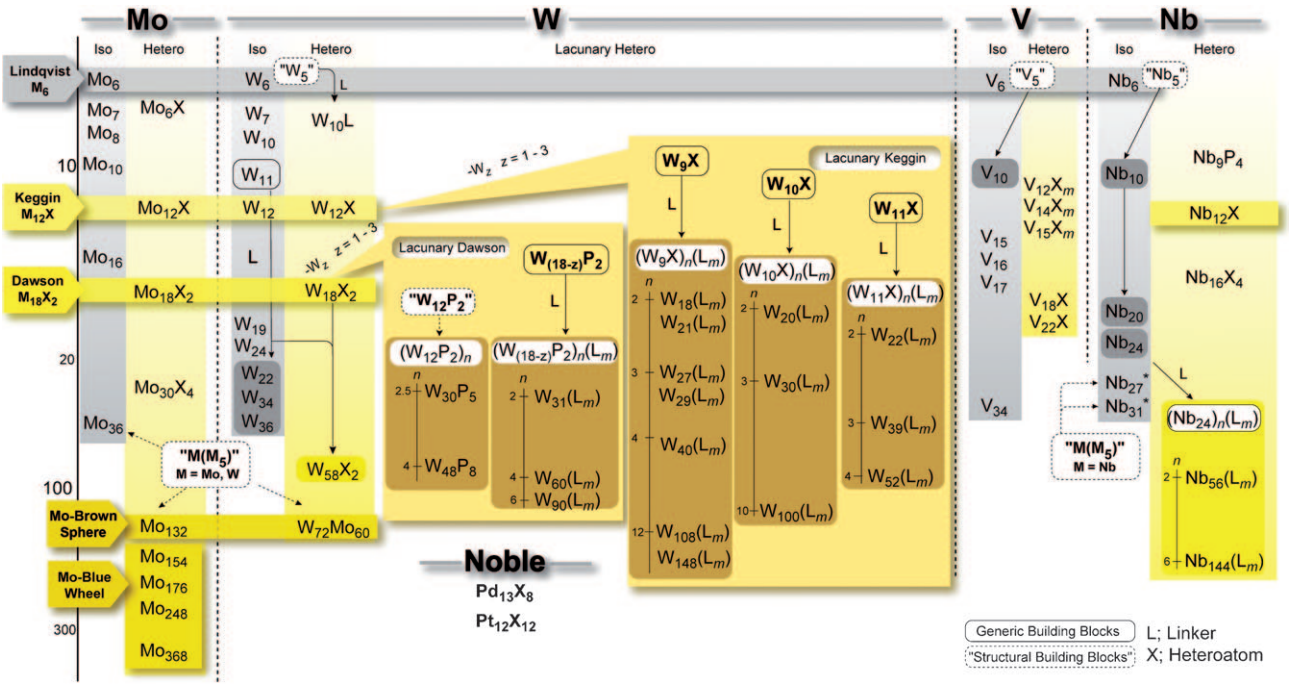

Figure 2. POM nuclearity using a classification based on building blocks of high-nuclearity clusters (Mo, W, V and Nb POMs).[1–13] The generic building blocks (in boxes with solid black lines) have been isolated as stable clusters: W_{11} isopolyanion, lacunary Keggin (W_9X, $W_{10}X$, $W_{11}X$), lacunary Dawson ($W_{(18-z)}P_2$), and Nb_{24} isopolyanions. These building blocks can be linked to form higher nuclearity clusters of nuclearity *n* by linkers L that contain a transition metal ion, alkyl metals, or heteroions. Thus $(W_9)_n(L_m)$ is composed of *n* W_9 building blocks assembled with several linkers of general formula L_m (the heteroatoms X are omitted here). Structural building blocks (in boxes with dashed lines) have not been isolated as clusters to date, but can be considered as building blocks for high-nuclearity POMs. These are: M_5 (one-metal lacunary Lindqvist; M = W, V, Nb), $W_{12}P_2$ (hexavacant lacunary Dawson), and $M(M_5)$ (pentagonal building blocks; M = Mo, W and Nb). Note: solid and dashed arrows do not correspond to synthetic routes. In a separate category are the noble metal POMs, where X = As for the Pd compound, and X = S for the Pt compound.

all empirically based, and an appreciation of the pH-dependent speciation of metalates can often be the key starting point in the synthesis. Generally, the approaches used to produce POM based clusters are simple, consisting of acidifying an aqueous solution containing the relevant molybdate and tungstate oxoanions (vanadates tend to be synthesized at high pH).[3] POM systems are complex owing to many thousands of combinatorially possible structure types, in which each building block can itself adopt a range of potential isomers.

Leroy (Lee) Cronin graduated in Chemistry in 1994 from the University of York, and obtained a DPhil. in bio-inorganic chemistry in 1997 under the supervision of Prof. P. H. Walton. After postdoctoral research at Edinburgh University with Neil Robertson and as an Alexander von Humboldt Research Fellow with Prof. A. Müller at the University of Bielefeld (Germany), he returned to the UK as a lecturer at the University of Birmingham in 2000. In 2002 took up a Lectureship in Glasgow; he was promoted to Reader in 2005, Professor in 2006, and was appointed to the Gardiner Chair of Chemistry in April 2009. He is a Fellow of the Royal Society of Edinburgh, Scotland's National Academy of Science and Letters.

Synthetically, the route to produce new POM clusters are often very simple synthetic manipulations requiring a small number of steps, or even just one step (one-pot syntheses; Figure 4). The acidification, for example, of a solution of sodium molybdate will give rise to metal oxide fragments, which increase in nuclearity as the pH of the solution decreases. This means that traditionally, the aqueous synthesis of the POM cluster is the norm, and as such can be in the presence of simple metal cations; however, this approach can be extended to organic cations, and the solvent system can be extended to an aqueous/organic solvent mixture; for example, water/CH_3CN. The synthetic variables of greatest importance in synthesizing such clusters are, in no particular order: 1) concentration/type of metal oxide anion, 2) pH, 3) ionic strength, 4) heteroatom type/concentration, 5) presence of additional ligands, 6) reducing agent, and 7) temperature of reaction and processing (e.g. microwave, hydrothermal, refluxing). In particular, the following recent developments in the synthesis of POMs can be used to search for new POM systems:

1) The use of protonated organic ammonium cations results in an inverse cation templation effect, which has been used to assemble new POM clusters,[10] hybrids,[14] and framework materials.[15]
2) The application of mixed-solvent strategies can lead to the isolation of new clusters, for example, a sulfite-based polyoxomolybdate[16] and $[(P_2O_7)W_{17}O_{51}]^{4-}$.[17]

 © 2010 Wiley-VCH Verlag GmbH & Co. KGaA, Weinheim

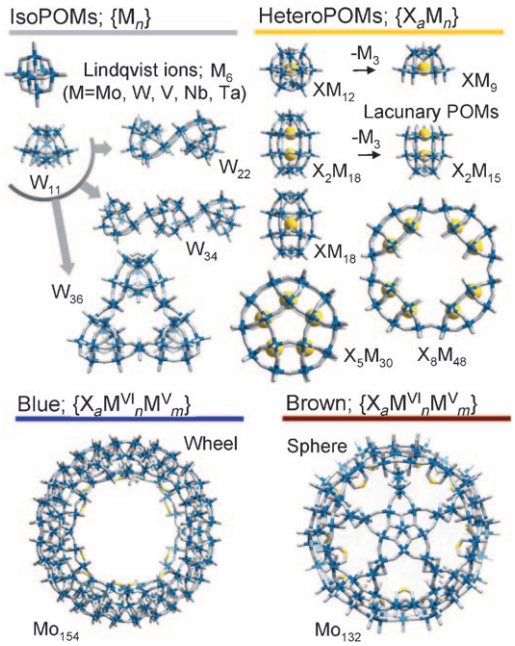

Figure 3. The principal broad POM subsets. The metal–oxygen framework is shown by sticks (M blue, O gray); heteroatoms are shown in yellow.

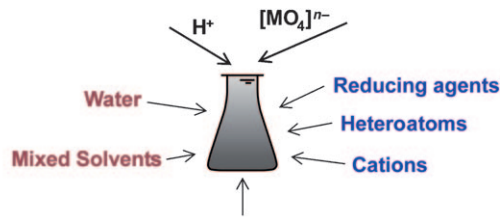

Figure 4. Parameters that are often adjusted in the synthesis/isolation of new POM clusters using the multi-parameter one-pot method.

3) Hydrothermal processing is becoming more popular and controllable, and in particular in the synthesis of POM-based coordination polymers.[18] However, microwave-based syntheses may yet prove more predictable than traditional hydrothermal syntheses.
4) The use of ionic liquids as solvent/cation directing species for the directed assembly of POMs. This is a new concept, with only one report to date.[19] Owing to their high polarity, ionic liquids have great potential for directed assembly, and this area is sure to expand.

2.2. Properties

2.2.1. Polyoxometallates Formed from Redox-Active Templates

Conventionally, redox-inactive anions, such as SO_4^{2-} and PO_4^{3-}, are often used as templating anions in the formation of many POM clusters. A strategy to create new functional POMs involves the encapsulation of redox-active templates instead. By utilizing sulfite, selenite, tellurite, and periodate anions as templates, several new types of redox-active heteroPOMs have been isolated. These POMs exhibit interesting thermochromic behavior or electrochemical properties that are related to the electron-transfer reactions within the clusters.[20,21] The POM cluster $[Mo_{18}O_{54}(SO_3)_2]^{4-}$, which contains two embedded redox-active sulfite templates, can be activated by a metallic surface and can reversibly interconvert between two electronic states.[16] Upon thermal activation, two electrons are ejected from the active sulfite anions and delocalized over the metal oxide cluster cage, switching it from a fully oxidized state to a two-electron reduced state. The hypothesis is that there is a concomitant formation of an S–S bond between the two sulfur centers inside the cluster shell (Figure 5).[16] This system is rather

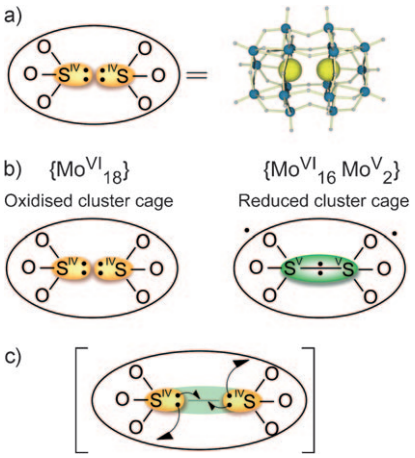

Figure 5. Hypothesized reversible S–S bond formation and electronic reorganization within the cluster cage. a) Right: The $[Mo_{18}O_{54}(SO_3)_2]^{n-}$ cluster framework (Mo blue, O gray, S yellow). Left: Abbreviated form containing the two SO_3^{2-} groups is shown in the ellipse. b) Left: starting state for the fully oxidized cluster; right: reduced state, in which the formation of the single S–S bond results in the movement of two electrons from the S atoms to the cluster cage, yielding $[\{Mo^V_2Mo^{VI}_{16}O_{54}\}(S^V_2O_6)]^{4-}$. c) The transition state in which the four electrons (depicted by arrows) rearrange, with two electrons forming the S–S bond and the remaining two reduce the cluster shell.

intriguing as it may be possible to build a type of field-effect transistor based upon single clusters of this type. By placing the cluster in a circuit and applying a potential to the base of the cluster, the internal redox centers could be activated, thus causing electron transfer and reduction of the cluster shell and thereby switching the electronic state of the cluster from the oxidized to the mixed-valence reduced state.[11,22]

Electrochemical investigations of $[Mo_{18}O_{54}(SO_3)_2]^{4-}$ show an extensive series of six one-electron reduction processes for both isomers of this cluster.[20] The tungstate analogues and one-electron reduced species $[W_{18}O_{54}(SO_3)_2]^{n-}$ have been synthesized and their electrochemical properties studied.[21] In a recent extension to this work, both templates could be replaced by a single template located in the center of the cluster to give a Dawson-like $\{W_{18}X\}$ POM.[23] The first member of this family to be discovered was actually an isoPOM $\{W_{19}\}$ with a Dawson-type cage; the nineteenth tungsten is located at the center of the cluster instead of the two tetrahedral heteroatoms that are usually found inside

 © 2010 Wiley-VCH Verlag GmbH & Co. KGaA, Weinheim

conventional Dawson clusters.[24] Structural analysis of the cluster shows that the nineteenth tungsten could be replaced by other elements, such as Pt^{IV}, Sb^{V}, Te^{VI}, or I^{VII}. The POMs $[H_3W_{18}O_{56}(IO_6)]^{6-}$ embedded with high-valent iodine[23] and $[H_3W_{18}O_{56}(TeO_6)]^{7-}$ that captures the tellurate anion TeO_6^{6-} were discovered thereafter (Figure 6).[25] It would be interesting to evaluate these new classes of Dawson-like clusters $\{W_{18}X\}$ as possible models for electron transfer from the bulk to the cage, and then from the cage to the internal heteroatom, because the redox potential of the heteroatom is clearly modulated by its local coordination environment. In the case of the reduction of Te^{VI} to Te^{IV}, it clearly requires a change in coordination from $\{O_6\}$ to $\{O_3\}$; formally, a $\{TeO_6\}^{6-}$ moiety is transformed into $\{TeO_3\}^{2-}$. As the cage effectively acts as a redox-active barrier between the external redox reagent and the internal redox-active guest, it will be of interest to understand how to control both the internal, cage, and coupled cage–guest redox processes.[25]

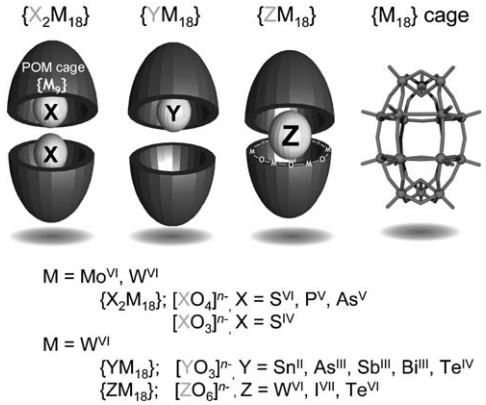

Figure 6. Embedding of heteroatoms in POMs. The ellipsoidal $\{M_{18}\}$ cages are split open to show the heteroatoms within. Right: The structure of the intact $\{M_{18}O_{54}\}$ cage.

This idea can be expanded, as the redox-active states associated with both the outside of the cluster shell and the internal heteroatom, which can be oxidized between Te^{IV} and Te^{VI} or I^{V} and I^{VII} in $[W_{18}O_{56}(XO_6)]^{n-}$ (X = I or Te) could be utilized as elements in molecular flash RAM. The internal reorganization of the template appears to be a relatively high energy process compared to the reduction and oxidation of the cluster shell. As such, these clusters will be excellent possible models for molecular flash RAM (Figure 7). Furthermore, the combination of an outside and an inside that can both exist in two separate states means that these cluster flash RAM candidates have at least four states in a single 1.4 nm cluster.

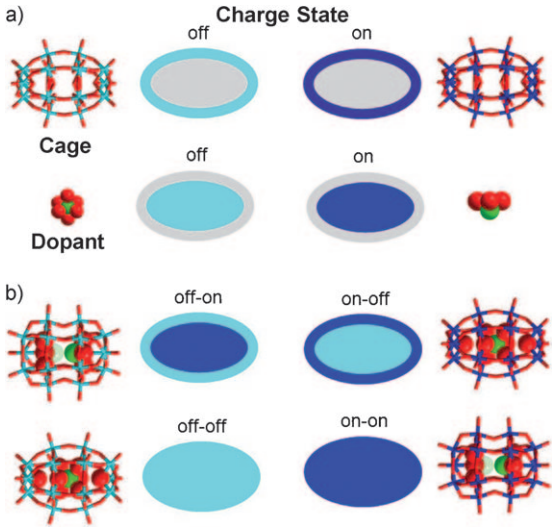

Figure 7. Proposed four-state flash-RAM. a) Cage and dopant: Left: oxidized (cyan); right: reduced (blue). b) The different combinations of oxidized guest and host (off–off) and reduced guest and host (on–on) along with the color-coded ellipses. Metal atoms: cyan or blue; oxygen: red; heteroatoms: green.

2.2.2. *Structures with Pentagonal $\{M_6\}$ Units*

Pentagonal building blocks in polyoxometalate cluster chemistry are needed to produce curved and spherical architectures in a similar fashion to the architectures of carbon nanostructures. This structural requirement has been reported for the wheel-like[12] $[Mo_{154}O_{462}H_{14}(H_2O)_{70}]^{14-}$ and ball-like Keplerate $[Mo_{132}O_{372}(CH_3COO)_{30}(H_2O)_{72}]^{42-}$ clusters.[13] It is important to realize the key role that pentagonal-type building groups play in the synthesis of these systems, and to consider how to ensure they are assembled in solution. Edge-sharing (condensed) pentagons cannot be used to tile a plane, whereas exactly 12 pentagons are required, in connection with well-defined sets of hexagons, to construct spherical systems, such as the truncated icosahedron, which is the most spherical Archimedean solid, commonly observed in polyhedral viruses, and in the geodesic Fuller domes. However, Sadakane et al. recently demonstrated that pentagonal units based upon $\{Mo_6\}$ can tile a plane if additional vanadate and antimonite linkers are incorporated into the structure (Figure 8).[26a] For tungstate-based clusters, a pentagonal $\{W_6\}$ has only very recently been observed in a $\{W_{72}Mo_{60}\}$-type species with 30 $\{Mo^{V}_2\}$ linkers and 12 pentagonal $\{W_6\}$ subunits, which are the first examples of pentagonal $\{W_6\}$ moiety in polyoxometalate chemistry, and this has also been extended to produce $\{(M)M_5\}_{12}Fe^{III}_{30}$ (M = Mo^{IV}, W^{VI}) Kep-

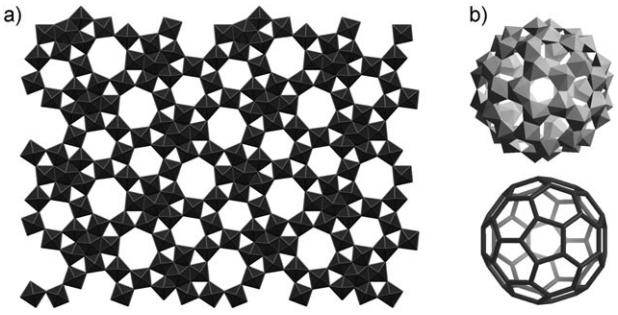

Figure 8. a) Polyhedral representation of orthorhombic Mo-V-Sb oxide in the *ab* plane with pentagonal $\{Mo_6\}$ units and linking $\{V_n\}$ polyhedra. The antimony centers occupy the hexagonal and heptagonal channels in the oxide.[26] b) Polyhedral representation (top) of $[UO_2(O_2)(OH)]_{60}^{60-}$ showing the cluster topologies (bottom). All uranium atoms are in the centers of the polyhedra.[28]

 © 2010 Wiley-VCH Verlag GmbH & Co. KGaA, Weinheim

lerate systems.[26b] These units are necessary for the formation of the spherical cluster like those of molybdenum analogues, and a structural link between giant molybdenum oxides and derived Keggin structures based on $[BW_{11}O_{30}]^{9-}$ with pentagonal units has been presented.[27] The realization that pentagonal units can generate curved structures allows the design principles to be extended. For example, elements such as uranium should be able to form structures that can incorporate hexagonal and pentagonal units; the uranyl ion, $\{UO_2\}^{2+}$ is able to coordinate to up to six additional ligands. This idea was recently demonstrated with a series of ball-shaped uranyl complexes with peroxo ligands. Among them, a $\{U_{60}\}$ cluster, $[UO_2(O_2)(OH)]_{60}^{60-}$, is topologically identical to C_{60}, with uranium centers located corresponding to carbon positions in C_{60} (Figure 8).[28]

The idea of designing pentagonal systems to ensure closure of a molecular system is not often discussed, yet it appears to be useful and straightforward in cluster chemistry. There are many analogies that can be made with fullerenes; owing to the nature of the coordinative interactions, mechanistic investigations of the self-assembly of spherical cluster systems containing pentagonal blocks could be extremely interesting, especially if attempts were made to trap or include template molecules within the sphere. Combining molybdenum and uranium chemistry has been discussed for use in nuclear waste remediation[29] by employing the ability of individual small atom building blocks to direct the assembly of large cluster spheres at low dilution.

2.2.3. Unconventional Polyoxometallate Clusters

The assembly of polyoxoniobates has mainly been focused on isopolyniobates, such as the $[Nb_6O_{19}]^{8-}$ Lindqvist ion. Recently, Nyman et al. reported the polyoxoniobate cluster $[Nb_{24}O_{72}H_9]^{15-}$,[30] which is derived from two fundamental structural types: the condensed octahedral $\{Nb_6\}$ ring and an open $\{Nb_6\}$ ring, which can serve as a building blocks for even larger clusters and extended structures.[31] We recently discovered some polyoxoniobates, $[HNb_{27}O_{76}]^{16-}$ and $[H_{10}Nb_{31}O_{93}(CO_3)]^{23-}$, that also incorporate pentagonal building units, and these clusters were assembled in the presence of a dibenzyldithiocarbamate; the reason for their formation is not yet known (Figure 9).[32]

Casey et al. reported the synthesis and characterization of a new type of POM structure, $[Ti_{12}Nb_6O_{44}]^{10-}$.[33] The super-Lindqvist cluster has six niobium centers located on the vertices of the octahedron and twelve titanium atoms on the middle point of each of the twelve edges. The remarkable feature is that there is a central cavity large enough to hold another niobium atom at the center of the cluster, but it is empty in this particular case. It may be possible to embed these clusters in titania and other oxides to produce novel materials based upon niobium oxides. It will be interesting to see if a range of new structures/processing approaches are adopted and if new physical properties for the normally inert niobium center can be found and exploited, especially given the new pentagonal structure architectures discovered and described by us above.[32]

Although the classification of POM clusters can be very helpful (Figure 2), the central paradigms are constantly being challenged as the result of new synthetic and structural developments. For example, the peroxo uranium compounds are certainly not classical POM clusters, but exhibit certain key similarities, especially to the larger structures.[28] Similarly, Kortz et al.[34] recently reported the first example of a molecular palladium oxide cluster, $[Pd^{II}_{13}As^{V}_{8}O_{34}(OH)_6]^{8-}$, which is a distorted cube with edge lengths of about 1 nm. This cluster comprises thirteen palladium(II) ions that have the square-planar geometry typical for Pd^{II}, in contrast to those of octahedral environments in all other discrete POMs. The Pd–O distances in the range 1.95–2.09 Å are normal for Pd–O single coordination bonds, and in this way the cluster could also be considered as a Pd^{II} complex of AsO_4^{3-}. Interestingly, although the Pd^{II} centers do not involve Pd=O moieties in this complex, it would appear that this cluster can be at least compared with POM-based structure types. Further developments in this field, for example replacement of the AsO_4^{3-} groups or even substitution of palladium for other metals, such as gold, will lead to a large variety of new structures (Figure 10). Although this structure has gained significant attention owing to potential for new developments, it should be noted that Wickleder et al. had presented a $[Pt_{12}O_8(SO_4)_{12}]^{4-}$ structure in 2004.[35]

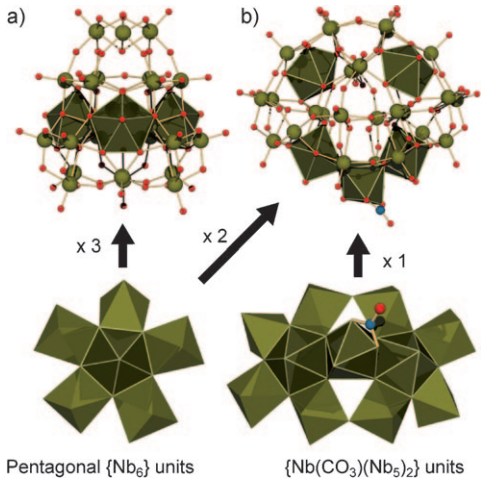

Figure 9. Structure of a) $[HNb_{27}O_{76}]^{16-}$ and b) $[H_{10}Nb_{31}O_{93}(CO_3)]^{23-}$ (Nb green, O red, C blue).

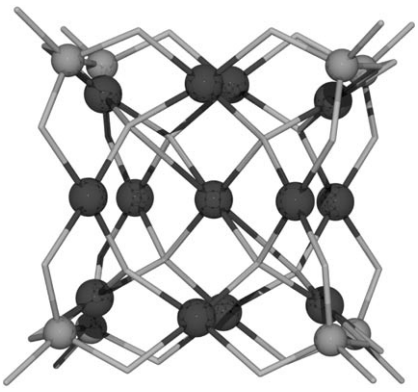

Figure 10. Structure of the $[Pd^{II}_{13}As^{V}_{8}O_{34}(OH)_6]^{8-}$ anion (Pd black spheres, As gray spheres, O gray sticks).

 © 2010 Wiley-VCH Verlag GmbH & Co. KGaA, Weinheim

From observations of Hill et al., it was suggested that POM clusters can act as strong π-acceptor ligands to stabilize late-transition-metal oxo groups, thus allowing the isolation of the first oxo complexes of the noble metals Pt, Pd, and Au. The Pt^{IV} complex $[O{=}Pt(H_2O)L_2]^{16-}$ ($L = [PW_9O_{34}]^{9-}$) received special attention, not only because this compound was a breakthrough with the late transition metals, but also because oxoplatinum intermediates are believed to be key participants in many oxidative processes occurring on platinum surfaces.[36] This compound is interesting as it challenges the concept of an oxo-wall,[37] and also raises real issues about the nature of the bonded configuration of the terminal oxo bound to the platinum[36] and in the related palladium[38] or gold compounds.[39] The stability of these compounds, and in particular the Pt=O moiety, has been the subject of discussion.[40] Milstein et al.[41] recently observed a platinum complex that appears to support a terminal oxo ligand similar to that of Hill,[36] but this species is quite reactive.

Apart from the oxo-based systems, new types of POM systems have been reported that incorporate peroxo-type ligands. Neumann et al. reported the isolation and characterization of a peroxide end-on $\{Fe^{III}\text{-}O_2\}$ POM-based compound in water with unusual properties.[42] The compound is stabilized by hydrogen bonding and is derived from a reaction between a POM with several iron(II) centers and H_2O_2. The structure contains a coordinate peroxo unit with an almost linear Fe-O-O unit and has been characterized by X-ray diffraction and electron energy-loss spectroscopy (Figure 11).[42] Conventionally the peroxide ligand adopts a

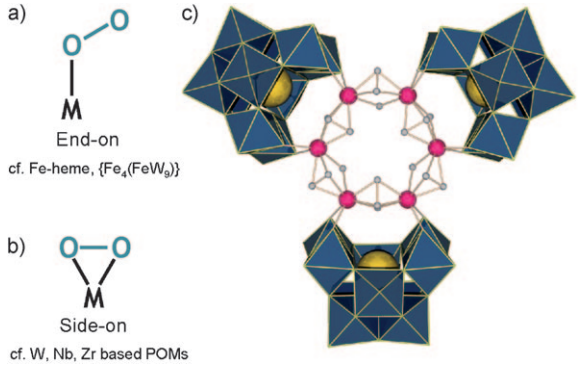

Figure 11. End-on (a) and side-on coordination (b) of peroxide ligands. c) Structure of 6-peroxo-6-zirconium crown $[Zr_6(O_2)_6(OH)_6(\gamma\text{-}SiW_{10}O_{36})_3]^{18-}$. W blue (polyhedra), Si yellow, O gray.

side-on, bridging coordination motif as found in the $\{(UO_2)\}_{60}$ structure and also in the 6-peroxo-6-zirconium crown $[M_6(O_2)_6(OH)_6(\gamma\text{-}SiW_{10}O_{36})_3]^{18-}$ (M = Zr, Hf).[28,43] These systems, which use highly charged POM ligands to stabilize reactive oxo, peroxo, or superoxide groups, are very important for the development of new catalysts, mechanistic insight, and structural motifs.[44]

2.3. Chirality in Polyoxometallates[45]

The large number of applications for POMs, which includes catalysis, biology, medicine, magnetism, material science, and photochemistry, means that there is considerable scope for the development of truly chiral metal oxide architectures. Chiral POM clusters have been formed from structural vacancies and geometrical distortions; however, such enantiomers are very easily racemized and are very difficult to separate and isolate. One strategy that may overcome these limitations would be to graft chiral organic ligands directly onto the POM framework.[45] Heterometallic ion linkers can be used to link chiral POM fragments to form chiral frameworks from the linkage of achiral units, for example by producing a twist between the linked POM anions, or the metal cation sandwiched between the two anions can coordinate in a distorted square-antiprismatic geometry.[46] The sandwich framework produced by linking the chiral POM building blocks can be either homochiral or heterochiral (meso); heterometal cations can mediate between the POM anions and organic molecules. For example, zirconium(IV) has been used to link the chiral tartrate and achiral lacunary Wells–Dawson POM unit, $\alpha\text{-}[P_2W_{15}O_{56}]^{12-}$ (Figure 12).[6] Recently, high-dimensional chiral

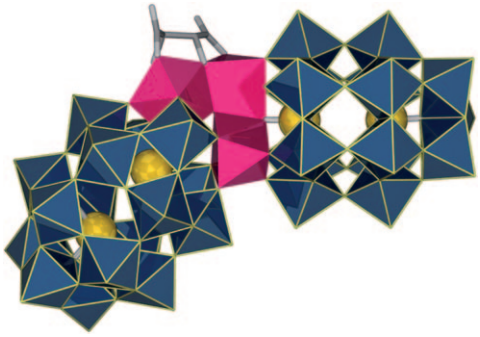

Figure 12. The structure of $[\alpha\text{-}P_2W_{15}O_{55}(H_2O)]Zr_3(\mu_3\text{-}O)(H_2O)(L\text{-}tartH)[\alpha\text{-}P_2W_{16}O_{59}]^{15-}$. P yellow, C gray sticks; polyhedra: W blue, Zr crimson.

frameworks have been formed by incorporating suitable achiral organic molecules, metal cations, and POM building units, even without any chiral auxiliaries. Furthermore, it is conceptually feasible to use complexes, such as $[Co(en)_2]^{3+}$, to partially substitute some molybdenum or tungsten atoms and lead to chiral motifs embedded in the clusters by replacing one of the bidentate ligands with the POM fragment itself. Indeed, the exploitation of the charge on the POM by using chiral cations could be very important to produce functional hybrids.[47]

As the key limitation of chiral POM research currently is that the enantiomers are easily interconverted and/or difficult to isolate, a common approach is to attempt resolution by employing chiral cations or to induce a Cotton effect. Statistically, between 5 and 10% of all racemated conglomerate crystals can be resolved spontaneously upon crystallization, and some chiral POMs can be formed using spontaneous resolution.[48–50] This area will certainly develop further, with the key goal being to form chiral POM metal frameworks that are well-defined, stable, and can be both detected and exploited, for example in chiral catalysis, sensing, or electronically active systems. One novel aspect may be to imprint

 © 2010 Wiley-VCH Verlag GmbH & Co. KGaA, Weinheim

the chiral features in the cluster by self-assembling the cluster using structure-directing chiral cations.[47] This approach extends the shrink-wrapping concept presented by us and allows intrinsically more structurally complex POM clusters to be assembled.[10]

2.4. Monitoring the Self-Assembly and Discovering New POM Clusters with Mass Spectrometry

Electrospray ionization mass spectrometry (ESI-MS) has been used extensively to investigate many types of polyoxometalates including vanadates, niobates, tantalates, chromates, molybdates, tungstates, and rhenates (see Ref. [51]). However, the availability of high-resolution detector systems has allowed the field to develop rapidly, because POMs complex isotopic envelopes resulting from the high number of stable isotopes of tungsten and molybdenum (4 and 7 respectively) and the clusters are intrinsically charged. This allows complete determination of the cluster formula down to the last proton by matching the calculated versus experimentally obtained envelopes, and mass spectrometry studies of unknown polyoxometalate systems have enormous potential to aid the discovery processes as well as allow studies to unravel the complex self-assembly mechanisms.

The difficulty associated with determining the protonation state of the cluster has been a major drawback to date of standard crystallographic XRD studies, which often do not provide direct information on the protonation state of the cluster anions. Therefore, mass spectrometry (MS) of polyoxometalates has the potential to become the standard analysis technique for complex cluster systems as it provides vital complementary information of the cluster composition in solution which cannot be deduced from crystallographic studies.[52–54] Furthermore, mass spectrometry can be used to probe mixed-metal clusters; for example, we have demonstrated the use of MS to authenticate the cluster composition of $\{Mo_{17}V_3\}$,[53] $\{W_{19}\}$,[24] $\{W_{18}I\}$,[23] to probe protonation versus heteroatom inclusion,[52] to identify new isopolyoxotungstates and functionalized POMs in solution,[54] to explore the formation of POM-based nanostructures,[55] and to look into the mechanism of POM self-assembly.[56] MS studies can also help in the synthesis of complex hybrid architectures, for example for the manganese Anderson POM cluster, $[N(C_4H_9)_4]_3[MnMo_6O_{18}(C_4H_6O_3NO_2)(C_4H_6O_3NH_2)]$, which is quite similar to the symmetrical counterparts when it is a $(NO_2)_2$ or $(NH_2)_2$ clusters, and especially when these two groups are disordered in the solid state. Mass spectrometry is useful in this case to establish separation methods for complex structure frameworks that may be synthetic intermediates, and fragmentation studies that look at the stability of the clusters.[57] Recently, Ma et al. have studied the fragmentation of a series of POM clusters in the gas phase. Together with common species from protonation, alkali metal ion association, and loss of water, the fragmented species $[W_xO_{3x+1}]^{2-}$ and $[PW_{12-x}O_{39-3x}]^-$ $(x=6–9)$ were observed. These results highlight the usefulness of ESI-MS in the characterization of complex POM anion clusters;[58] the reaction mechanism of polyoxoniobates with hydrogen peroxide has also been investigated using ESI-MS.[59]

In recent work, we have employed cryospray mass spectrometry (CSI-MS) to investigate unstable POM complexes[56] and examine the reaction mechanism. Cryospray ionization mass spectrometry is useful as it allows the temperature of the infused solution and resulting electrospray to be controlled, thus allowing temperature-controlled mass spectrometry. This method is useful in general, because the examination of labile, weak, or non-covalent interactions had precluded analysis by other ionization techniques, such as fast atom bombardment (FAB), matrix-assisted laser desorption ionization (MALDI), and electrospray ionization (ESI) owing to dissociation of the species. The technique is therefore of interest for investigations of labile POM systems because previous ESI-MS studies of such systems have been limited by the use of low resolution detectors and the high temperatures utilized in the ESI process (Figure 13).

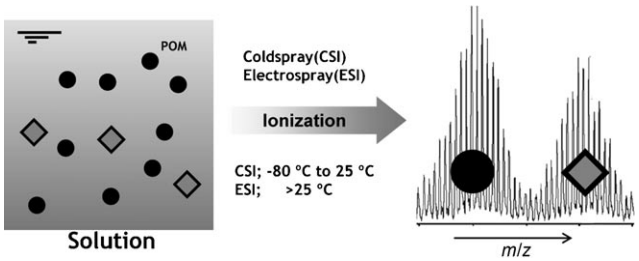

Figure 13. ESI and CSI mass spectrometry in the investigation of complex isotopic systems, such as POM-based molecules.

Using CSI-MS, we were recently able to screen new cluster systems to establish whether tellurium can be embedded as a heteroanion into a Dawson-like cluster cage, and also to monitor the in-situ reduction of Te^{VI} to Te^{IV}.[25] This new approach to the discovery of nanoclusters with cage templates utilizes cryospray mass spectrometry to directly probe the reaction solution, thereby allowing the process to be accomplished much more quickly, and it allows the discovery of new guests inside nanocluster cage architectures (Figure 14).

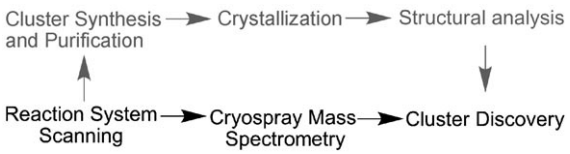

Figure 14. Comparison of conventional three-step cluster characterization with the one-step cryospray mass spectrometry approach.

3. POM Nanostructures and Nanocomposities

The fact that POMs have a high charge, well-defined structures, and are based upon conserved building blocks, and that they form by self-assembly, means that they have great potential to span multiple length scales. For instance, the $\{Mo_{154}\}$ wheel cluster, self-assembled at low pH under reducing conditions from Na_2MoO_4, can undergo a further self-assembly process to form vesicle-like structures com-

 © 2010 Wiley-VCH Verlag GmbH & Co. KGaA, Weinheim

posed of circa 1200 $\{Mo_{154}\}$ wheel-shaped clusters in solution.[60] Similarly, the cluster ball, $\{Mo_{72}Fe_{30}\}$, also undergoes a self-assembly process to form spherical heteropolyoxometalate $\{Mo_{72}Fe_{30}\}$-based macroions that form into single-layer vesicles 50–60 nm in diameter.[61] Along with electrostatically assembled structures, the assembly of lacunary structures to a size of many nanometers can be achieved using transition metal linkers, and nanoparticle assembly can be mediated by POMs. In this section we explore the incredible variety of structures, length scales, and control that can be achieved using POM-based building blocks (Figure 15).

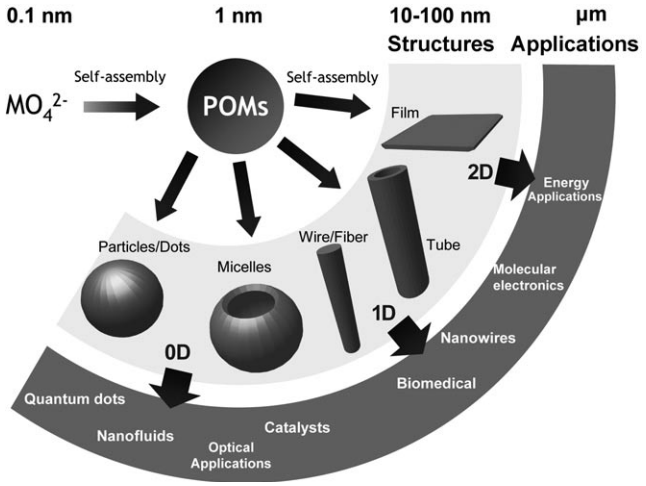

Figure 15. POM clusters (ca. 1–5 nm in size) assembled from mononuclear metalate ions (ca. 0.1 nm of size) can also act as building blocks for nanoscale structures (10–100 nm) by template-mediated and electrostatic self-assembly. These materials range from zero-dimensional particles and micelles, one-dimensional tube and wire structures, to two-dimensional thin films.

3.1. Hybrid Organic–Inorganic Polyoxometalate Architectures

Given the exceptional physical and structural properties intrinsic to POM superstructures, the ability to covalently modify the metal oxide cage in a reliable and predefined manner holds promise for the development of molecular materials that bridge the gap between molecular organic and bulk semiconducting oxides. Recently, Proust et al. have published an extensive review of POM–organic hybrids.[62] Herein, we will cover some illustrative examples ranging from the Lindqvist to the Dawson structure types.

The functionalization of the Lindqvist anion is well-documented; the $\{Mo_6\}$ cluster can be functionalized by replacing Mo=O groups with Mo=N−R moieties.[63] Not only the terminal oxo group can be substituted; recently Wei et al. found that the bridging oxo groups can also be replaced by amine groups.[64] For example, in $[Mo_6O_{14}(NAr')_5]^{2-}$ four terminal and one bridging oxo ligand can be replaced by imine moieties, and a ligand-free palladium-catalyzed Heck reaction of aryl iodides and bromides can be used to graft alkenes to hexamolybdate. By "diluting" the olefinic units, which are normally easily accessible and tend to polymerize, this method offers a route for the Heck reaction to occur in a more controllable and rational way.[65] Ligation onto both sides of manganese Anderson clusters with tridentate ligands can be used to add large organic aromatic groups, such as pyrene, symmetrically and asymmetrically on two sides of the cluster.[57,66] Grafting of C_6, C_{16}, and C_{18} alkyl chains onto manganese Anderson clusters, along with metathesis to exchange the cations with dimethyldioctadecylammonium (DMDOA), results in the formation of new POM assemblies with the hydrophilic POM cores enclosed by surfactant of DMDOA.[67]

The Dawson-type cluster $\{P_2V_3W_{15}\}$ can also be grafted with an organic moiety by chelation of a tridentate ligand to the $\{V_3\}$ trimer cap.[55] Hasenknopf et al. have reported a series of POM hybrids of the type $[P_2V_3W_{15}O_{59}\{(OCH_2)_2C(Et)NHCOR\}]^{5-}$, which are the first examples of the insertion of amides into a POM framework cage. The feature of these hybrids is the substitution of a POM oxo bridging ligand with the carbonyl oxygen of the amide group (Figure 16). Variation of the amide residue allowed efficient

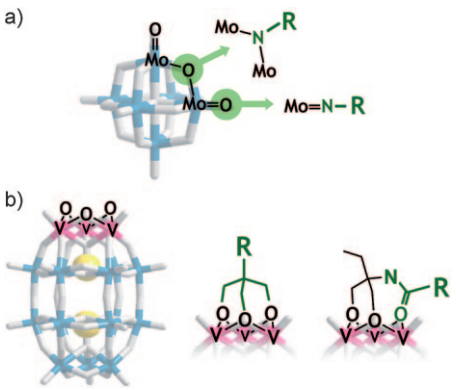

Figure 16. Extension of Lindqvist (a) and Dawson POMs (b) by covalent connections with organic groups. Functionalized organic moieties are shown as R.

electronic communication between the organic ligand and the inorganic cluster, which is reflected in the changes of redox properties of the hybrid POM. Conversely, the electron-accepting properties of the POM are transmitted to the ligand, which could be used to tune the organic part and help the design of POM-based redox sensors.[68] Furthermore, POM hybrids grafted to aromatic systems could be used to look at efficient charge separation for light-harvesting applications. For example, Odobel et al. covalently attached a perylene monoimide unit onto a $\{P_2W_{17}\}$ cluster, whereby the organic chromophores undergo electron transfer reactions with the POM cluster under illumination, as the hybrid forms a relatively long-lived radical anion.[69] Finally it must be mentioned that POM frameworks can be functionalized by organoantimony moieties, which themselves bridge between two sandwiching $\{W_9\}$ clusters in $[\{PhSbOH\}_3(A\text{-}\alpha\text{-}PW_9O_{34})_2]^{9-}$.[70]

3.2. Highly Condensed Superstructures

3.2.1. Isopolyoxtungstate Clusters as Building Blocks

Nanoscale POM structures can be assembled from heteroPOM subunits; however, isoPOM building blocks are

© 2010 Wiley-VCH Verlag GmbH & Co. KGaA, Weinheim

rarely used, presumably owing to their more labile and unstable nature. Despite this fact, we have recently isolated and characterized several related isopolyoxotungstate clusters,[3,54,71,72] namely $[H_4W_{22}O_{74}]^{12-}$, $[H_{10}W_{34}O_{116}]^{18-}$, and $[H_{12}W_{36}O_{120}]^{12-}$, thus demonstrating a new building-block principle that can be generated using pure isopolyoxotungstate-based on $\{W_{11}\}$ units (Figure 17). The $[H_4W_{22}O_{74}]^{12-}$

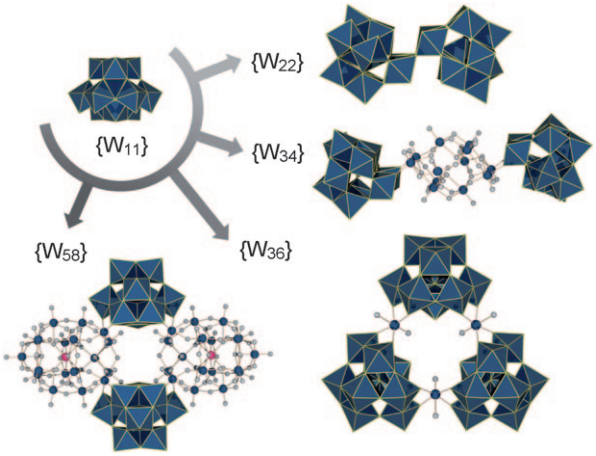

Figure 17. Assembly of $\{W_{22}\}$, $\{W_{34}\}$, $\{W_{36}\}$, and $\{W_{58}\}$ cluster structures. The $\{W_{11}\}$ unit is highlighted in the polyhedral representations; other linkers are shown in ball and stick representations (W blue, O gray, Te pink).

cluster is formed from two $\{W_{11}\}$ units, and $[H_{10}W_{34}O_{116}]^{18-}$ is formed from two $\{W_{11}\}$ units and a $\{W_{12}\}$ unit. That these clusters are relatively stable was demonstrated by mass spectrometry studies, which showed the presence of the molecular ions. The $[H_{12}W_{36}O_{120}]^{12-}$ ion can be considered as the aggregation of three $\{W_{11}\}$ units and three $\{W_1\}$ units. Also, we have synthesized a W–Te superstructure in which a $\{W_{58}\}$ cluster is observed; it can be regarded as the product of condensation from two tellurium-centered Dawson clusters and two $\{W_{11}\}$ clusters.[25] Further to this, Kortz et al. have shown that the $\{W_{22}\}$ cluster can act as a tridentate ligand and coordinate to two Ln^{3+} ions to form metal complexes, which have been fully characterized.[73]

3.2.2. Heteropolyoxometalate Lacunary Clusters as Building Blocks

The most convenient way to assemble molecular nanosized POM architectures is by the ligation of heteroPOM lacunary clusters by complexation with electrophiles or additional heteroatoms. For example, the super-tetrahedral cluster $[KFe_{12}(OH)_{18}(\alpha\text{-}P_2W_{15}O_{56})_4]^{29-}$ is formed by four trilacunary Dawson clusters $\{P_2W_{15}\}$ linked by a $\{Fe_{12}\}$ core in solution. Mass spectrometry was used to investigate the reaction system, and revealed the existence of the 16 kDa tetramer cluster species in solution; crystallographic studies showed that it is a 2.6 nm sized tetrahedral complex (Figure 18).[74] The formation of a large heterochiral POM architecture, the "cluster of clusters" $[\{\alpha\text{-}P_2W_{15}O_{56}\}_6\{Ce_3Mn_2(\mu_3\text{-}O)_4(\mu_2\text{-}OH)_2\}_3(\mu_2\text{-}OH)_2(H_2O)_2(PO_4)]^{47-}$, was presented

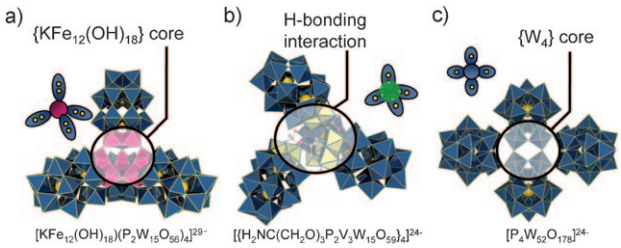

Figure 18. Nanoscale POM structures formed from lacunary heteroPOMs. Polyhedral units (circled): W blue, Fe purple, V light yellow. Insets: simplified view of the structures.

by Kögerler et al. This structure is assembled from multiple molecular components that are based on the trivacant Dawson polyoxotungstate $[\alpha\text{-}P_2W_{15}O_{56}]^{12-}$.[75a] Remarkably, the construction of such a highly negatively charged and aggregated POM is directed by the much smaller phosphate anion. Using the same trivacant precursor $[\alpha\text{-}P_2W_{15}O_{56}]^{12-}$, the authors obtained a high-oxidation-state cluster $[\{\alpha\text{-}P_2W_{16}O_{57}(OH)_2\}\{Ce^{IV}Mn^{IV}_6O_9(O_2CCH_3)_8\}]^{8-}$,[75b] thus demonstrating a straightforward route for grafting redox-active POM building blocks to existing manganese carboxylate clusters and for modeling their deposition onto metal oxide surfaces. Boskovic et al. reported a synthetic strategy for polynuclear lanthanoid complexes to produce high-nuclearity POM-encapsulated gadolinium and ytterbium complexes from $\{AsW_9\}$ subunits,[76] and a dumbbell-shaped POM, $[Re_2(PW_{11}O_{39})_2]^{8-}$, can be prepared from two $\{PW_9\}$ subunits. The structure of this complex contains a central core comprising a quadruple $\{Re_2\}$ bonded species with a Re–Re bond distance of 2.25 Å; this moiety is coordinated by two $\{PW_9\}$ units.[77] Furthermore, an actinide POM hybrid, a U-shaped $\{P_8W_{36}\}$ cluster incorporating uranyl peroxo units, has also been reported.[78] The POM lacunary units act as building blocks that can be joined together to form nodes, and this approach is becoming more reliable and may allow targeted design approaches to be adopted. In this context, the polyoxometalate periodic table (Figure 2) could be a very useful starting point for the systematic design of new POM-based architectures.

Clusters can also be built up by a disassembly–reassembly approach. For example, we recently reported the pH-controlled assembly of a nanoscale $[P_4W_{52}O_{178}]^{24-}$ cluster at pH 2 and its disassembly to a $[P_3W_{39}O_{134}]^{19-}$ cluster species at pH 2–3, a $[P_4W_{44}O_{152}]^{20-}$ cluster at pH 3–5, and finally $[P_2W_{19}O_{69}(OH_2)]^{14-}$ at pH 6. This process can be observed in the solid state, and also in solution using dynamic light-scattering studies.[79] The assembly of weakly associated clusters by H-bonding interactions has been achieved for the protein-sized tetramer, $[\{H_2NC(CH_2O)_3P_2V_3W_{15}O_{59}\}_4]^{24-}$, which is assembled from four $[H_2NC(CH_2O)_3P_2V_3W_{15}O_{59}]^{6-}$ clusters by H-bonding interaction between amino and methylene protons and cluster oxo ligands in solution (Figure 18). These weakly bonded superstructures can be characterized using CSI mass spectrometry.[56] The fact that the large hydrogen-bonded tetrahedron can be both observed in solution and crystallized means that it may even be possible to extend the mass-spectrometry studies from cluster discovery to controlling the

 © 2010 Wiley-VCH Verlag GmbH & Co. KGaA, Weinheim

self-assembly of superstructures in solution before crystallization.

3.2.3. Composites of Large Cations and Anions

Another way to build nanostructured POM-based architectures is to use large metal complex cations as counterions. In one example, the trinuclear Ru^{III} cation $[Ru_3O(OAc)_6(CH_3OH)_3]^+$ with Keggin-type $\{GeW_{12}\}$ and $\{SiMo_{12}\}$ and the Wells–Dawson-type $\{P_2W_{18}\}$ units can be used to form large cation–anion composite materials with solvent-accessible voids. In these architectures, both components can be tuned to afford a different function.[80] Large ionic crystal structures with different alkali metal ions can be formed from Keggin-type POMs $[\alpha\text{-}XW_{12}O_{40}]^{n-}$ (X = P, Si, B, Co) and the trinuclear cation $[Cr_3O(OAc)_6(H_2O)_3]^+$. The cavity volumes of the ionic crystals formed by desorption of solvated water vary with the nature of the alkali metal ions included. Such porous materials can be used for the selective sorption and successful separation of mixtures of alcohols, nitriles, esters, and water.[81] The next step would be to organize catalytically active cations and anions for the selective sorption and chemical transformation of the sorbed material. Similar approaches with cesium–crown ether complex cations have been used to form large cation–anion composites. A highly directed system is defined by the coordination of the Mo=O moiety of a Keggin ion with the cesium ion located within the crown cavity to give a crystalline solid complex $[Cs([18]crown\text{-}6)]_3H_2[PMo_{12}O_{40}]$. In this complex, the Keggin cluster is reduced by two electrons; the cesium ion is at the center of the [18]crown-6 bound to an $\alpha\text{-}[PMo_{12}O_{40}]^{5-}$ axle and the Mo=O units are coordinated to the crown ether units. Two rotation frequencies for the [18]crown-6 units are observed in temperature-dependent ^1H NMR spectroscopy studies, and these are dominated by intermolecular interactions in the solid state.[82]

This approach has been extended to use cationic dyes to form photoactive POM-based materials. Salts of the pararosaniline dye cation and the $[S_2Mo_{18}O_{62}]^{4-}$ sulphate Dawson cluster anion and Keggin clusters $\{MW_{12}O_{40}\}$ (M = Co, Zn) show significant perturbation of the ion electronic states of the dye that are induced by charge-assisted N–H···O hydrogen bonds to the POM cluster.[83] An important class of hybrid molecular conductor based upon POM building blocks can be formed from segregated stacks of the π-electron-donating tetrathiafulvalene (TTF) molecules as counterions. Coronado et al. recently reviewed the crystal engineering of such materials, and highlighted their magnetic and electronic properties.[84] Thus size-matching of large cations with POM-based anions can lead to novel materials with functionalities that can reflect both the cationic and anionic building blocks.

3.3. Multi-Dimensional Coordination Polymers

Given their charge, vast range of available building blocks, and accessible symmetries, POM-based units make exceptional candidates for the development of coordination polymers. However, this potential and versatility also means that there have been literally hundreds of POM coordination polymers flooding the literature with metal–organic building blocks giving rise to POM-based MOF like systems; however, these reports focus on novel topologies rather than functionality. One interesting approach involves the use of POMs in the assembly of all-inorganic frameworks. The silver POM family, which we recently discovered,[85] is based upon the well-studied silver(I)-octamolybdate $[Mo_8O_{26}]^{4-}$ combination. In solution, the system initially forms discrete $[Ag\{Mo_8\}Ag]$ precursor units, which can be identified by mass spectrometry and crystallized out using a range of different cations.[56] The self-assembly of these units to form dimeric $\{Ag_2\}$ linkers leads to the isolation of chains and networks in which the $[Mo_8O_{26}]^{4-}$ clusters are cross-linked by silver(I) cations. The influence of the solvent on the overall topology and the role of the counterion on the resulting structure have been established in each case. Fine-tuning of the metal–metal distances of the dimeric $\{Ag_2\}$ linking units can be achieved by using different coordinating solvents, which act as bridges. In some cases, the silver centers are so distant that no interaction is found between them in the crystal lattice.[86]

There are also reports on the coordination polymers of the silver/tungsten POM system, including a Keggin cluster-based open framework constructed from unsupported Ag···Ag interactions.[87] X-ray structural studies showed that the two principal subunits, protonated α-metatungstate clusters $[H_3W_{12}O_{40}]^{5-}$ and dimeric $\{[Ag(CH_3CN)_2]_2\}^{2+}$ bridging units, are linked such as to enclose two sets of parallel channels. Tetrahedrally symmetric $[Ag(CH_3CN)_4]^+$ units are located in the channels, and appear to act as templates in the self-assembly of the framework (Figure 19).

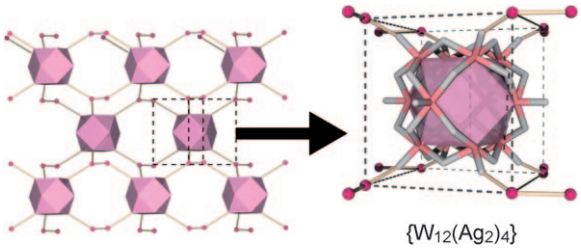

Figure 19. The principal cubic coordination environment. $\{W_{12}\}$ clusters (pink polyhedra) are linked to eight Ag bridges (red spheres) to form an open framework structure that is assembled by unsupported Ag···Ag interactions.

There are many other types of coordination polymers formed through transition metal linkers. The structure $[\{Ln(H_2O)_6\}_2As_8V_{14}O_{42}(SO_3)]$ ($Ln = La^{3+}$, Sm^{3+}, Ce^{3+}) from Das et al. is an example in which each POM cluster links to six $[Ln(H_2O)_6]^{3+}$ complex cations, and each $[Ln(H_2O)_6]^{3+}$ cation is coordinated to three surrounding POM cluster anions to form a two-dimensional layer structure; in this system, the POM cluster captures a sulfite anion.[88] An all-inorganic framework was recently presented that is formed by the isolation of the Keggin net, $[(C_4H_{10}NO)_{40}(W_{72}M_{12}O_{268}X_7)_n]$ ($M = Mn^{III}$, X = Si, $C_4H_{10}NO$ = morpholinium), which is a rare example of a three-dimensional framework made up

© 2010 Wiley-VCH Verlag GmbH & Co. KGaA, Weinheim

purely of POM building blocks through direct W–O–M coordination bonds.[15] In the native material, the Mn^{III} centers occupy the lacunary cavities of the Keggin clusters, so the Mn^{III} ions profoundly affect the redox properties of the solid.

The three-dimensional Keggin net framework $[W_{72}M_{12}O_{268}X_7]^{40-}$ ($M = Mn^{III}$, $X = Si$)[15] incorporates active sites that are capable of undergoing a reversible redox process involving the simultaneous inclusion of ascorbic acid as reducing agent with a concerted and spatially ordered reduction of the framework giving rise to the first example of a crystalline material that is able to reversibly undergo single-crystal to single-crystal redox transformations, whereby the (re)oxidation can be achieved with peroxoacids (Figure 20). Remarkably, this reversible redox process can

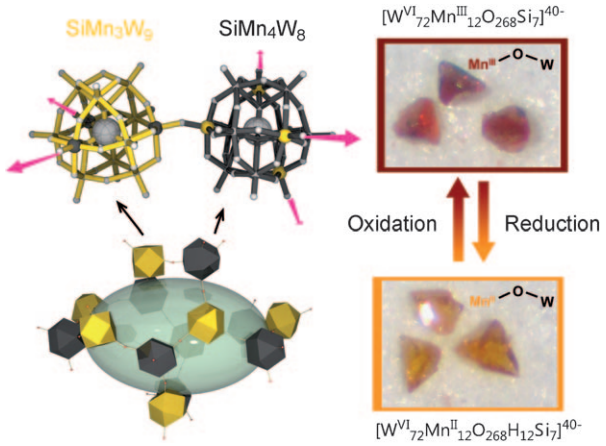

Figure 20. The 3D framework of $[W_{72}M_{12}O_{268}Si_7]^{40-}$. The network is built from two types of lacunary Keggin clusters that act as either 3-connected (yellow) or 4-connected (black) nodes. The ball-and-stick representation of the clusters (top) shows how the secondary building units (SBUs) are linked into an infinite 3D framework. A nanosized pocket (dimensions: $2.7 \times 2.4 \times 1.3$ nm^3) is indicated by the ellipsoid. Photographs show the single-crystal to single-crystal redox processes.

be tuned by changing the heteroatom template within the Keggin net from silicon to germanium.[89] This new class of inorganic framework materials bridges the gap between coordination compounds, metal–organic frameworks, and solid-state oxides (Figure 20).[15]

Coordination polymers can form through the combination of complexes with spacer ligands and POMs, which act as templating/complex counterions located in the cavities of the polymer to balance the charge. For example, Liu et al. have used the hydrothermal reaction of copper nitrate, benzentricarboxylate (btc), and different Keggin POMs to produce a number of crystalline solids $[(CH_3)_4N]_2[Cu_2(btc)_{4/3}(H_2O)_2]_6[H_nXM_{12}O_{40}]$ ($X = Si$, Ge, P, As; $M = W$, Mo).[18] In these compounds, the Keggin clusters are confined in the cavities of the Cu-btc-based metal-organic framework host matrix as non-coordinating guests (Figure 21). The typical acid catalysis performance of $\{PW_{12}\}$-containing compounds was assessed with the hydrolysis of esters in excess water, which showed high catalytic activity, reproducibility, and selectivity for substrate size. The well-dispersed POM clusters prevents them conglomerating and deactivating, which thus enhances their catalytic properties.[18] By changing the spacer length of the organic ligands, the dimensionality of the coordination polymer based on the POM can be tuned (Figure 21).[90]

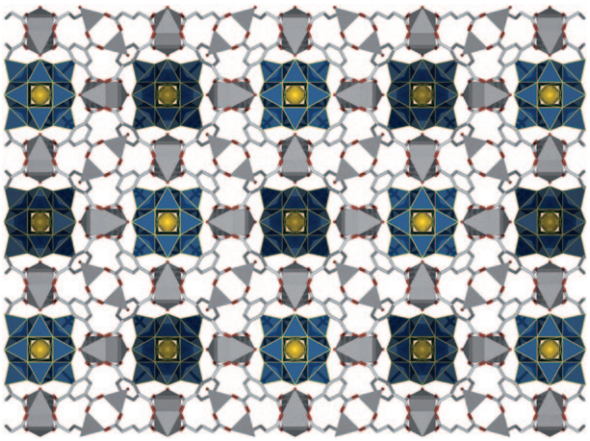

Figure 21. $[Cu_2(btc)_{4/3}(H_2O)_2]_6[H_nXM_{12}O_{40}]$, which contains Keggin ions as non-coordinating guests within a framework. W blue, X yellow, O red, C gray, Cu gray polyhedra.

3.4. Thin Films on Surfaces

An important aspect of POMs is their solubility in a variety of solvents, which places POMs in a unique position as soluble metal oxides. Therefore, it is possible for the compounds to form stable and well-ordered films, for example cast films, Langmuir–Blodgett (LB) films,[91–94] or layer-by-layer (LbL) film assemblies (Figure 22).[22,95–99] Their

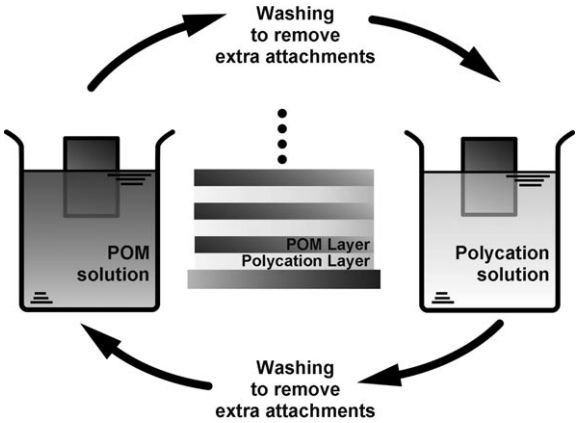

Figure 22. LbL film fabrication.

redox, chromic, magnetic, conducting, and catalytic properties mean that POMs are candidates for applied systems ranging from advanced catalysts to electronic devices.[96]

The LB process can be used to fabricate multilayer films with wet techniques; for example, hybrid films of $\{PMo_{12}\}$

 © 2010 Wiley-VCH Verlag GmbH & Co. KGaA, Weinheim

with organic cations can be made that show reversible coloration–decoloration properties.[91] Gao et al. have reported that the layer-by-layer (LbL) self-assembly of films of dye–POM composites (Keggin-type $[BW_{12}O_{40}]^{5-}$ and the sandwich complex $[Co_4(H_2O)_2(PW_9O_{34})_2]^{10-}$) with a cationic dye. The self-assembly into the films depends on hydrogen-bonding between the amine group in the dye cation and oxo groups of POMs, and on electrostatic interactions. The films showed high thermal stability and potential for dye-sensitized photocatalysis activity under visible light irradiation.[95] LbL films of $(NH_4)_{14}[NaP_5W_{30}O_{110}]$ and poly(4-vinylpyridine) (P4VP), in which P4VP plays both roles of immobilizing the POM and proton reservoir needed for the photochromic response, show electrochromic and photochromic properties. Photo- and/or electrochemical stimulation induces a color change in the LbL film from colorless to blue.[97] Einaga et al. reported a novel type of thin film with surface properties that are controllable by UV irradiation in aqueous solution. The photochromic multilayer film was made using the LbL method from the Preyssler-type POM $\{NaP_5W_{30}\}$ and polyethyleneimine (PEI). The outermost PEI layer could be detached by UV irradiation in aqueous solution and recovered by subsequent dipping into a PEI solution. Photopatterned films can thus be prepared by image-wise UV exposure with highly site-selective adsorption.[98]

POMs can also be assembled on surfaces, using microcontact printing, by stamping self-assembled monolayers (SAMs) onto a gold surface that present the correct functionalities for further reaction with the incoming cluster. Using this approach, we studied the interactions between the human fibroblast (hTERT-BJ1) cells and pyrene groups covalently grafted on unsymmetrical manganese Anderson POM clusters that form a micropatterned monolayer. The cells attach and spread more efficiently for these kinds of hybrid monolayer than a pure pyrene monolayer or POM cluster monolayer, selectively adhering only to the SAM–Anderson–pryene conjugate on a gold surface.[100]

The electronic properties of LbL molecular films of the Keggin POM $[H_3PW_{12}O_{40}]$ with 1,12-diaminododecane on 3-aminopropyltriethoxysilane-modified silicon surfaces have also been investigated. The electron transport properties were characterized using 50 and 150 nm electrode gaps for films consisting of one or five layers. A conduction mechanism was suggested that involves Fowler–Nordheim tunneling and percolation mechanisms.[22]

3.5. Self-Assembly of POM Nanostructures

In the previous sections, we have focused on the aggregation of POMs at the molecular level; in this section however we will discuss the assembly of POMs across larger length scales. These nanostructures[101] are normally formed by supramolecular interactions and are much less ordered; POMs that have been derivatized to form amphiphile-like molecules can be effectively self-assembled into such structures. We have observed that the manganese Anderson $C_{16/18}$, an anionic POM cluster covalently connected with two C_{16} or C_{18} alkyl chains, can slowly assemble into membrane-like vesicles. In the vesicles, hydrophilic manganese Anderson clusters orientate towards the outside of the shell layer, and long hydrophobic alkyl chains stay inside to form the solventophobic layer (Figure 23). This system is the first example of hydrophilic POM macroions used as polar head groups for a surfactant system.[67,102] Wu et al. reported onion-like structures of a surfactant-encapsulated and stabilized POM system.[103]

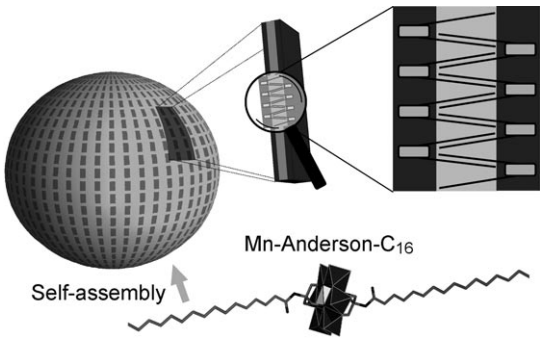

Figure 23. The manganese Anderson–C_{16} surfactant and their vesicle formation. The inorganic manganese Anderson structure is shown with polyhedra, and the organic part is presented with sticks (Mn gray polyhedra; Mo–O blue polyhedra; C gray sticks; N dark gray, O light gray). In the schematic view (top right), the black lines denote the C_{16} alkyl chains.

Apart from these assembly structures, which are stabilized by organic cations (Table 1), pure inorganic salts of POM and small inorganic cations can form self-assembly structures that comprise a spherical layer, which were named blackberries by Liu et al.:[60] nanoscale, water-soluble macro-ions, such as $\{Mo_{132}\}$, $\{Mo_{154}\}$, $\{Mo_{72}Fe_{30}\}$, and others, tend to form stable, uniform, single-layer blackberry structures 20–1000 nm in size in dilute solutions by noncovalent interactions.[104,105] Two interesting features of Keplerate $\{Mo_{72}Fe_{30}\}$ blackberries are that 1) they create a microscaled, relatively isolated water environment (containing over three million water molecules) that has different properties from the bulk water, and 2) the blackberry membrane is permeable to small cations, but not to anions. The passive transport of cations across the blackberry membrane is relatively slow but does not need any carrier or additional energy.[106]

The formation of these large supramolecular structures seems to be a general phenomenon. The major driving force for the formation of blackberries appears to be a counterion-mediated attraction. Monovalent counterions play an important role in the self-assembly of macroions, possibly providing an attractive force contributing to blackberry formation, and not van der Waals forces or hydrophobic interactions that are well-known as a driving force for vesicle self-assembly.[107] The size of the blackberries can be predicted from the zeta potential and the cohesive bond energy.[108] The equilibrium size is determined by their renormalized charge density, which in turn is regulated by counterion condensation. This leads to the prediction that the size of the shells grows linearly with the inverse of the dielectric constant of the medium.[108]

© 2010 Wiley-VCH Verlag GmbH & Co. KGaA, Weinheim

Table 1: Recent reports as examples on low-dimensional self-assembly nanostructures fabricated by POMs with their size and component structures.[a]

	Morphology	POM	Feature	Ref.
0D	Particles, dots	Keggin; $H_{3+x}PV_xMo_{12-x}O_{40}$ (x = 0, 2)	micelle-directed nanoparticles	[109]
		$[(H_4PVW_{17}O_{62})]$	polyoxometalate-capped Pd- nanoparticles	[110]
		$(DODA)_4SiW_{12}O_{40}$	onion-like particle	[103]
		Anderson POM substituted by a long alkyl chain	membrane-like vesicles in MeCN/water	[102]
		$K_{12}Li_{13}[Cu_{20}Cl(OH)_{24}(H_2O)_{12}(P_8W_{48}O_{184})]$	"blackberries"	[107]
1D	tubes	$(HTyr)_3PMo_{12}O_{40}$, $(HTyr)_3PW_{12}O_{40}$, etc.	Salts with protonated amino acids (HTyr, HPhe, HThr, Trp) forms nanotubes and also nanoparticles and rods	[111]

[a] Tyr = tyrosine, DODA = dimethyldioctadecylammonium.

4. Engineering Functionality: From Molecules to Materials

4.1. Redox Properties

The ability to configure or tailor redox properties is one of the most important features for POM compounds, and provides a major motivation in the development of new functional systems. The Dawson cluster $\{Mo_{18}O_{62}X_2\}$ can be readily sixfold reduced without any change in the cluster geometry. Furthermore, the redox properties for the same type of clusters can be tuned by incorporating different heteratoms or replacement of one metal ion on the cluster shell. For example, Dawson-type POMs disubstituted with phenylphosphonate, phenylsilyl, or *tert*-butylsilyl moieties can accept up to five electrons, and the organic substituents modify the first and second reduction potential of the POM relative to the unsubstituted ion $[P_2W_{18}O_{62}]^{6-}$. The presence of phenylphosphonate lowers the reduction potential, whereas the phenylsilyl or *tert*-butylsilyl moieties causes cathodic shifts.[112] The Preyssler anion, $[M^{n+}P_5W_{30}O_{110}]^{(15-n)-}$, is able to accept electrons at low potentials, to selectively capture various metal cations M^{n+}, and to undergo acid–base reactions. Calculations to evaluate the energetics of the release/encapsulation process for several M^{n+} cations and to identify the effect of the encapsulated ion on the properties of the Preyssler anion shows a linear dependence between the first one-electron reduction energy and the encapsulated X^{n+} charge, with a slope of 48 mV per unit charge. The protonation also shifts the reduction potential to more positive values, but the effect is much larger.[113] This extends to POM-based materials, and as discussed above, the three-dimensional Keggin net framework incorporates active sites that are capable of undergoing a reversible redox process involving the simultaneous inclusion of the reductant with a spatially ordered redox change of the framework (Figure 20). Further development of these frameworks by inclusion of cobalt ions should lead to highly redox-active materials.

Because POMs have variable redox potentials, they are excellent candidates as synthons and catalysts. Recently, Nadjo et al. reviewed the synthesis of extremely stabilized metal nanostructures using POMs that act as both reducing and capping agents. Two main strategies were summarized for the preparation of the reduced POMs used in the synthetic process: one by photochemical reduction, and the other by direct synthesis. Indeed, this process has been featured as a green synthesis of metal-based nanostructures.[114]

Recently, Wu et al. developed a method to anchor both silver or gold nanoparticles (NPs) and Preyssler-type POMs in a silica matrix. The metal NPs are synthesized from the adsorption and in situ reduction of metal ions in the silica matrix by the reduced POMs that are produced by irradiation in the presence of amines. The thin film prepared from a silica matrix containing POMs and NPs exhibits both the transparent and easily processible properties of matrix and the stable and reversible photochromism of POMs. The size and location of NPs can be tuned by controlling the adsorption time of metal ions and mask blocking the surface. Materials prepared in this way have potential applications in optical displays, memory units, catalysis, microelectronic devices, and antibacterial materials.[115] $H_3PW_{12}O_{40}$-assisted electrochemical reduction of CCl_4 or C_2Cl_4 can produce single-walled carbon nanotubes and carbon nanosheets and related nanostructured carbons; $H_3PMo_{12}O_{40}$-assisted electro-etching of graphite followed by simple ball milling of the etched-off powder can produce a large quantity of larger "onion-like" carbon nanostructures. Both the electrochemical reduction and ball milling process were carried out under ambient air conditions; this process can be readily scaled up for mass production.[116] POMs have great potential as optical materials; for example, the study of reversible redox-switchable second-order optical nonlinearity for the POM cluster $[PW_{11}O_{39}(ReN)]^{n-}$ ($n = 3$–7) has been achieved using the time-dependent density functional theory (TDDFT) method combined with the sum-over-states (SOS) formalism.[117]

4.2. Magnetic POMs

Polyoxometalate clusters have a diverse range of electronic properties arising from the ability to form a range of reduced species. This feature, combined with the ability to act as well-defined ligands for polynuclear transition metal clusters, means they have great potential for the discovery and design of new molecular magnetic devices. For example, the $[PMo_{12}O_{40}(VO)_2]^{n-}$ cluster has been described as an important model compound as a possible spin qubit, because the redox-active core unit of the Keggin cluster is capped on opposed positions by two V=O species, each containing

 © 2010 Wiley-VCH Verlag GmbH & Co. KGaA, Weinheim

localized spin s = 1/2. It was then hypothesized that these two spins can be coupled through the electrons of the central core by electrical manipulation of the molecular redox potential owing to the change of charge.[118] The fact that POMs can be intrinsically electronically/redox active is one of the major strengths of POM-based ligands, especially in magnetic systems, as it offers an additional route by which the exchange pathways and electronic configuration of the system may be controlled.

Although the magnetic properties of polyoxovanadates have been well-studied, new aspects continue to be discovered; a recent example includes the theoretical study on the fully localized spin cluster of $[(V^{IV})_{18}O_{42}]^{12-}$ and its spin-delocalized mixed-valence species $[V^{IV}{}_{10}V^{V}{}_{8}O_{42}]^{4-}$, which were described based upon the structure of $Cs_{12}[V_{18}O_{42}(H_2O)]$.[119] Furthermore, a series of compounds, $[V_6O_6(OCH_3)_8(calix)(CH_3OH)]^-$ anions (calix = *p-tert* butylcalix[4]arene) were synthesized using several organic cations (Et_4N^+, NH_4^+, PyH^+, Et_3NH^+) by solvothermal reactions in methanol. The Lindqvist core was partially reduced, and the composition of these clusters was shown to be $\{V^{III}V^{IV}{}_5O_{19}\}$, thus indicating a mixed-valence state. These compounds were the first polyoxovanadate(III,IV) with a Lindqvist-type structure, and ferromagnetic $V^{IV}\cdots V^{III}$ interactions were revealed by magnetic measurement.[120]

Sandwich-based polyoxometalates in which a metal core is capped by POM ligands are extremely popular in the literature, as it is possible to introduce magnetic species into the POM using a designed approach (Table 2). Azido POM compounds with Mn^{III} and Cu^{II} as paramagnetic centers were reported, in which an 1,3-bridging N_3^- ligand acts as a linker between two $[(\gamma\text{-}SiW_{10}O_{36})Mn_2(OH)_2]^{4-}$ units and two $[(\gamma\text{-}SiW_{10}O_{36})Cu_2(N_3)_2]^{6-}$ subunits connected through the two μ-1,1,1-azido ligands, with the four paramagnetic centers forming a lozenge. The azido ligands have different coupling properties depending on their conformation: end-to-end and end-on 1,3-bridging and terminal coordination modes tend to lead to antiferromagnetic ferromagnetic coupling.[121] Other copper(II) clusters, such as the sandwich-type POM cluster $\{Cu_8(GeW_9)_2\}$, show weak ferromagnetic exchange interactions among the copper(II) centers.[122] In the sandwich-type POM $\{Cu_4(GeW_9)_2\}$, quantum tunneling at zero field is suggested from the asymmetric magnetization between a positive and a negative pulsed field at 0.5 K on the hysteresis loop.[123]

We reported one of the first examples of a polyoxometalate-mediated single-molecule magnet (SMM), $[(GeW_9O_{34})_2\{Mn^{III}{}_4Mn^{II}{}_2O_4(H_2O)_4\}]^{12-}$ (Figure 24), in which a central cationic mixed-valance hexameric manganese core is stabilized by two POM ligands. Despite the complex and distorted nature of the cationic core, these architectures are very stable. The tetrahedral oxo ligands involved in the coordination to the transition metal cationic core are important to the ideal tunable units to control/modify the physical properties of the entire molecule.[126] Other SMMs have also been reported, for example, the $[ErW_{10}O_{36}]^{9-}$ anion, in which one erbium ion is encapsulated by two $\{W_5\}$ ligands (Figure 24). The molecule is an inorganic analogue of the bis(phthalocyaninato)lanthanide SMMs; both molecules have similar coordination/ligand field symmetries around the central erbium ion where the distorted cubic coordination was also stabilized by the POM ligand, here the $\{W_5\}$ ligand.[127]

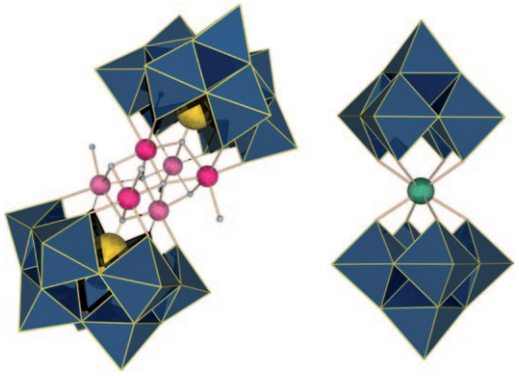

Figure 24. Structures of single-molecule magnets based on POMs: $[(GeW_9O_{34})_2(Mn^{III}{}_4Mn^{II}{}_2O_4(H_2O)_4]^{12-}$ anion (left) and $[ErW_{10}O_{36}]^{9-}$ anion (right).

Table 2: Sandwich POMs and their magnetic properties.

POM	Magnetic features	Magnetic building block	POM building block	Ref.
$[(\gamma\text{-}SiW_{10}O_{36})_2Cu_4(\mu\text{-}1,1,1\text{-}N_3)_2(\mu\text{-}1,1\text{-}N_3)_2]^{12-}$	ferromagnetic interactions between the four Cu^{II} centers, $S=2$	$Cu_4(N_3)_4$	SiW_{10}	[121]
$[\{(\gamma\text{-}SiW_{10}O_{36})Mn_2(OH)_2\text{-}(N_3)_{0.5}(H_2O)_{0.5}\}_2\text{-}(\mu\text{-}1,3\text{-}N_3)]^{10-}$	antiferromagnetic interaction with a diamagnetic ground state, $S=1$	$Mn_4(N_3)_2$	SiW_{10}	[121]
$[Cu(H_2O)_2]H_2[Cu_8(dap)_4(H_2O)_2(\alpha\text{-B-}GeW_9O_{34})_2]$	weak ferromagnetic exchange interactions among the Cu^{II} centers	$\{Cu_8\}$	GeW_9	[122]
$[Cu_4(GeW_9O_{34})_2]^{12-}$	hysteresis loop at 0.5 K indicates the quantum tunneling at zero field	$\{Cu_4\}$ tetragon	GeW_9	[123]
$[(\beta\text{-}SiFe_2W_{10}O_{37}(OH))(\gamma\text{-}SiW_{10}O_{36})]^{13-}$	antiferromagnetic exchange between the two $s=5/2$ Fe^{III} centers	$\{Fe_2\}$	$(SiW_{10}O_{37}(OH))$ and $(\gamma\text{-}SiW_{10}O_{36})$	[124]
$K_{14}Na_{17}[(Mn^{III}{}_{13}Mn^{II}O_{12}(PO_4)_4(PW_9O_{34})_4]$	antiferromagnetic interaction in the $\{Mn_{14}\}$ core	$\{Mn_{14}\}$	$[PW_9O_{34}]$	[125]
$\{[XW_9O_{34}]_2[Mn^{III}{}_4Mn^{II}{}_2O_4(H_2O)_4]\}$	SMM[a]	$\{Mn^{III}{}_4Mn^{II}{}_2\}$	XW_9O_{34} (X = Ge, Si)	[126]
$[ErW_{10}O_{36}]^{9-}$	SMM[a]	Er	W_5	[127]

[a] SMM = single-molecule magnet.

© 2010 Wiley-VCH Verlag GmbH & Co. KGaA, Weinheim

5. Catalytic Applications in Green Chemistry and Energy Systems

The use of polyoxometalate clusters as catalysts continues to be the most popular application area for POMs, and in particular by industry, with hundreds of papers and many patents published every year covering this topic. Many reviews cover the progress of POM chemistry in this aspect, including recent reviews on the development of green H_2O_2-based epoxidation systems,[128] catalytic oxidation of organic substrates by molecular oxygen and hydrogen peroxide by multi-step electron-transfer, a biomimetic approach,[129] progress and challenges in POM-based catalysis and catalytic materials chemistry,[130] and catalytic strategies for sustainable oxidations in water.[131] For the purposes of this review, we will only focus on important results published during the last two years (Figure 25 and Table 3).

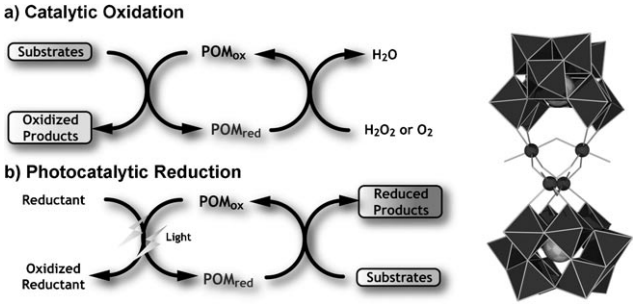

Figure 25. POM-catalyzed reaction systems: a) catalytic oxidation reaction and b) photocatalytic reduction. Right: Structure of the $[\{Ru_4O_4(OH)_2(H_2O)_4\}(\gamma\text{-}SiW_{10}O_{36})_2]^{10-}$ anion (W gray polyhedra, Ru dark gray spheres, Si light gray).

5.1. Water Splitting

Efficient catalytic water splitting is an important area of research, and in particular for the utilization of solar energy (especially if the water splitting system can be embedded into photoelectrodes). Studies have been carried out on the suitability of many catalysts. For example, a redox-active tetraruthenium POM $[\{Ru_4O_4(OH)_2(H_2O)_4\}(\gamma\text{-}SiW_{10}O_{36})_2]^{10-}$ (Figure 25) combined with either a cerium(IV)[132] or $[Ru(bipy)_3]^{3+}$ catalyst was found to catalyze the rapid oxidation of H_2O to O_2 in water at ambient temperature, and shows considerable activity.[133] This step is thermodynamically the hardest part of the water-splitting process. To complete the process, the conversion of protons into hydrogen is required, thus the design of a POM-based hydrogen-evolving complex would be interesting, and the design of a bifunctional system that could catalyze both processes would be even better.

5.2. Catalysis with POMs

A crown-ether complex cation $[Pd^{II}\{(H_3O)[15]crown\text{-}5\text{-}phen\}Cl_2]^+$ (phen = phenanthroline) and $[H_4PV_2Mo_{10}O_{40}]^-$ anion can catalyze Wacker alkene oxidation, in essentially quantitative yields, using N_2O instead of O_2 as oxidant.[148] A hybrid carbon nanotube–POM can electrocatalytically oxidize methanol when the POM-modified carbon nanotube electrode was coated by Pt/Ru nanoparticles,[140] and the mechanism and kinetics of ether and alkanol cleavage catalyzed by POMs have been examined.[149] Phosphodiester bond cleavage by a POM was reported using the heptamolybdate anion $[Mo_7O_{24}]^{6-}$; the reaction rate was accelerated by four orders of magnitude.[141,142] Ester hydrolysis in water can be greatly enhanced by the catalysis of the POM, $H_3PW_{12}O_{40}$, immobilized on organomodified mesoporous silica. This design overcomes the difficulty involved with the use of solid acids by which catalytic activity is often severely deactivated by water.[150] The one-pot hydrogenolysis of glycerol to the diol can be achieved with 96% selectivity to 1,2-propanediol (1,2-PDO) at 21% of glycerol conversion using a $Cs_{2.5}H_{0.5}[PW_{12}]$ catalyst with 5 wt% of ruthenium to give an active bifunctional catalytic system.[143] The dicopper-

Table 3: Important POM-catalyzed reactions reported since 2006.

System	POM	Ref.
water splitting	$[\gamma\text{-}SiW_{10}O_{36}]^{8-}$	[132]
	$Rb_8K_2[\{Ru_4O_4(OH)_2(H_2O)_4\}(\gamma\text{-}SiW_{10}O_{36})_2]$	[133]
alkene oxidation	$[PW_{11}CoO_{39}]^{5-}$ and $[PW_{11}TiO_{40}]^{5-}$	[134]
	$[C_{21}H_{37}N]_2[(PhPO_3)\{WO(O_2)_2\}_2\{WO(O_2)_2H_2O\}]$	[135]
	$[C_{21}H_{37}N]_2[(p\text{-}NO_2Ph(O)PO_3)\{WO(O_2)_2\}_2\{WO(O_2)_2H_2O\}]$ (higher activity than above)	
	$[bmim]_3PW_{12}O_{40}$[a]	[136]
	V_xPMA[b] ($x = 1$–3)	[137]
alcohol oxidation	$[\alpha\text{-}SiV^VW_{11}O_{40}]^{5-}$ or $[\alpha\text{-}SiMn^{III}W_{11}(H_2O)O_{39}]^{5-}$	[138]
	Pt^0 nanoparticles stabilized by $H_5PV_2Mo_{10}O_{40}$	[139]
	POM-modified carbon nanotubes	[140]
phosphodiester hydrolysis	$[Mo_7O_{24}]^{6-}$	[141,142]
hydrogenolysis of glycerol to 1,2-propanediol	$Cs_{2.5}H_{0.5}[PW_{12}O_{40}]$	[143]
photochemical decomposition of $C_2F_5OC_2F_4OCF_2COOH$	$H_3PW_{12}O_{40}$ and $H_4SiW_{12}O_{40}$	[144]
oxidative homocoupling of alkynes	$TBA_4[\gamma\text{-}H_2SiW_{10}O_{36}Cu_2(\mu\text{-}1,1\text{-}N_3)_2]$	[145]
intramolecular cyclization of (+)-citronellal	$Cs_8[(\gamma\text{-}SiW_{10}O_{36})_2\{M(H_2O)\}_4(\mu_4\text{-}O)(\mu\text{-}OH)_6]$ (M = Zr or Hf)	[146]
oxidation of hydrocarbons	$Fe(salen)Cl\text{-}SiW_{11}O_{39}$	[147]
hydrolysis of esters	$[Cu_2(btc)_{4/3}(H_2O)_2]_6[H_nXM_{12}O_{40}]\cdot(C_4H_{12}N)_2$ (X = Si, Ge, P, As; M = W, Mo)	[18]

[a] bmim = 1-butyl-3-methylimidazolium hexafluorophosphate. [b] PMA = phosphomolybdic acid.

 © 2010 Wiley-VCH Verlag GmbH & Co. KGaA, Weinheim

substituted γ-Keggin silicotungstate, $TBA_4[\gamma\text{-}H_2SiW_{10}O_{36}Cu_2(\mu\text{-}1,1\text{-}N_3)_2]$ (TBA = tetra-*n*-butylammonium), is catalytically active in the oxidative alkyne homocoupling and formation of diynes from alkynes in good yields.[145] Di- and tetranuclear metal-sandwich silicotungstates $[(\gamma\text{-}SiW_{10}O_{36})_2M_2(\mu\text{-}OH)_2]^{10-}$ and $[(\gamma\text{-}SiW_{10}O_{36})_2M_4(\mu_4\text{-}O)(\mu\text{-}OH)_6]^{8-}$ (M = Zr or Hf) show catalytic activity for the intramolecular cyclization of (+)-citronellal to isopulegols without formation of byproducts; it was suggested that the $[M_4(\mu_4\text{-}O)(\mu\text{-}OH)_6]^{8+}$ moiety acts as an active site for the cyclization process.[146] The dialuminium-substituted silicotungstate $TBA_3H[\gamma\text{-}SiW_{10}O_{36}\{Al(OH_2)\}_2(\mu\text{-}OH)_2]\cdot 4H_2O$ is catalytically active in the intramolecular cyclization of (+)-citronellal and 3-methylcitronellal without formation of by-product.[151] Furthermore, the POM-encapsulated metal–organic framework $[Cu_2(btc)_{4/3}(H_2O)_2]_6[H_nXM_{12}O_{40}]\cdot(C_4H_{12}N)_2$ (X = Si, Ge, P, As; M = W, Mo), in which the POM is alternately arranged without coordinative interactions, shows acid catalytic activity in the hydrolysis of esters, and selectivity depending on the molecular size of substrates and their accessibility into the pore surface.[18]

5.3. Polyoxometalate-Functionalized Electrodes

A $H_3PW_{12}O_{40}$-modified titania hybrid electrode with a tailored microstructure has been studied for its photoelectrochemical applications. The encapsulation of a POM inside TiO_2 nanotubes results in a much better modification effect and chemical stability than the rough aggregation of POMs on the surface of a multiporous TiO_2 film. Furthermore, applying an external anodic potential to TiO_2/Ti or POM-TiO_2/Ti electrodes can enhance the photodegradation efficiency of bisphenol A.[152] The oxygen reduction reaction (ORR) of a series of transition-metal-substituted Wells–Dawson $[P_2W_{17}M^nO_{62}]^{(12-n)-}$; $M = W^{VI}$, Fe^{II}, Co^{II}, Ru^{II}) and Keggin $[PW_{12}O_{40}]^{3-}$ and $[PCoW_{11}O_{39}]^{5-}$) anions was investigated at gold, palladium, and platinum electrodes. The positive shifts of the ORR potential depend on the transition metal. A $[PCoW_{11}O_{39}]^{5-}$ co-catalyst and a platinum cathode shows best performance.[153] Fuel cells that operate with solutions of reduced POM $\{PMo_{12}\}$ can remove CO gas (from ethylene glycol decomposition in systems) by oxidizing it to CO_2, and $[PMo_{12}O_{40}]^{3-}$ was reduced to $[PMo_{12}O_{40}]^{5-}$.[154]

5.4. Biological Activity of Polyoxometalates

Although many polyoxometalates can be considered to be the ultimate "inorganic" molecules, their well-defined size, configurable charge, and ability to produce organic–inorganic hybrids means that they have great potential to interact with biomolecules. In recent years, a number of studies have been carried out employing POMs as anticancer and anti-viral agents (see Table 4 for a brief summary of some of this recent research). Significant antitumor activity of a reduced POM $[Me_3NH]_6[H_2Mo^V{}_{12}O_{28}(OH)_{12}(Mo^{VI}O_3)_4]$ was reported by Yamase et al.,[155] and the effect on the growth of cancer cell lines and xenografts was assessed by a cell viability test and analysis of tumor growth. $[NH_3iPr]_6[Mo_7O_{24}]\cdot 3H_2O$ was found to be particularly effective in some tumors showing activity against Co-4 (human colon cancer), MX-1 (human breast cancer), and OAT (human lung cancer). This cluster also demonstrated growth suppression for MKN-45 human gastric cancer in tumor-bearing mice.[156] Further experiments showed that the antitumor activity was due to apoptosis.[157] The origin of the biological effect is not understood, but it is interesting to note that POMs have been found to be effective CK2 inhibitors in terms of both efficiency and selectivity, and they are nonclassical kinase inhibitors (protein kinase CK2 is a multifunctional kinase that is disregulated in many cancers).[158]

Table 4: Recent reports on the biological uses of POMs.

Antiviral activity	POM	Ref.
cancer	$[iPrNH_3]_6[Mo_7O_{24}]$	[156, 157]
replication of herpes simplex virus	$K_7[PTi_2W_{10}O_{40}]$	[159]
influenza virus (FluV) A		
respiratory syncytial virus activities	$[iPrNH_3]_6[PTi_2W_{10}O_{38}(O_2)_2]$	[160]
RNA virus (FluV A, RSV, parainfluenza virus (PfluV) type 2, dengue fever virus, HIV-1, and SARS)	$K_{10}Na[(VO)_3(SbW_9O_{33})_2]$, $K_{12}[(VO)_3(AsW_9O_{33})_2]$	[160]
MRSA and VRSA cells	$K_6[P_2W_{18}O_{62}]$, $K_4[SiMo_{12}O_{40}]$, $K_7[PTi_2W_{10}O_{40}]$	[161]

A number of POMs have been tested for the anti-RNA viral activity and have been proven to be broad spectrum and nontoxic anti-RNA virus agents that are promising candidates for first-line therapeutics in acute respiratory diseases.[160] The Keggin cluster ($K_7[PTi_2W_{10}O_{40}]6H_2O$; PM-19) has the ability to prevent the interaction between the herpes virus entry mediator and the herpes simplex virus envelope protein.[159] Enhancement of antibacterial activity of β-lactam antibiotics by methicillin-resistant and vancomycin-resistant *Staphylococcus aureus* was observed for $[P_2W_{18}O_{62}]^{6-}$, $[SiMo_{12}O_{40}]^{4-}$, and $[PTi_2W_{10}O_{40}]^{7-}$.[161] $H_3PW_{12}O_{40}$, $H_3PMo_{12}O_{40}$, and $H_4SiW_{12}O_{40}$ can photocatalytically inactivate *Escherichia coli* (Gram-negative) and *Bacillus subtilis* (Gram-positive); they thus form a homogeneous photocatalytically active system that is more efficient and faster than that of heterogeneous TiO_2 photocatalysts. The biocidal properties of such POM photocatalysts may be utilized in the future as disinfectant technologies.[162]

The interaction between POMs and general biological systems also have attracted interest, and it has been demonstrated that biopolymer POM interactions are significant in the gelatin–decavanadate system.[163] Such systems provide a simple and efficient way for the development of homogeneous functional bionanocomposites involving naturally occurring polymers, and POMs embedded in cations can be useful agents for interacting with viruses.[164] Furthermore, proteins can ligate a remarkable variety of POMs that are formed from the interaction between proteins and molybdates/tungstates;[165] the complexation of POMs by human serum albumin[166] has been carried out with $[H_2W_{12}O_{40}]^{6-}$ and

© 2010 Wiley-VCH Verlag GmbH & Co. KGaA, Weinheim

$[NaP_5W_{30}O_{110}]^{14-}$. Therefore, it should not be surprising that POMs can even help manipulate/control the folded structure of prion proteins.[167]

6. Summary and Outlook: Polyoxometalates and the Emergence of New Phenomena

Research on polyoxometalates is entering an exciting new phase that is moving beyond the synthesis and structural characterization of new cluster systems. The development of functional composites that utilize the intrinsic chemical and electronic properties, size, and self assembling aspects promises to lead to increasingly sophisticated molecular systems that could be utilized as devices with many programmable functions. The arrangement of a range of functions into a hierarchy could allow the design of new materials from the ground up that exploit the transferable building blocks found in polyoxometalate chemistry.

For example, polyoxometalate clusters show promise as components in multifunctional nanomaterials, such as carbon-based nanostructures, and it has even been possible to image the sterically regulated translational and rotational motion of discrete tungsten POM Lindqvist ions (i.e., $[W_6O_{19}]^{2-}$) within carbon nanotubes.[168] The nanoscale confinement of molecules has been shown within complex polyoxometalate Keplerate clusters in which 12 pentagonal $[(Mo^{VI})Mo^{VI}_5O_{21}(H_2O)_6]^{6-}$ ligands are connected by 30 $[Mo^{V}_2O_4(OAc)]^{+}$ spacers. This cluster has a very well-defined surface in which the spacers contain 20 Mo_9O_9 rings that are about 3 Å in diameter (from the van der Waals radii of opposing O atoms); these spaces allow access to the large internal cavity (Figure 26). The Mo_9O_9 rings serve as pore-like openings to

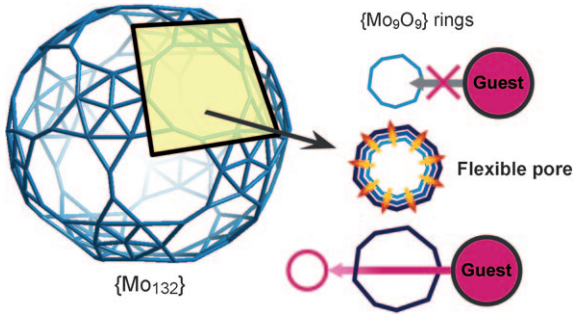

Figure 26. Keplerate POM with Mo_9O_9 rings, which act as flexible pores, highlighted in yellow.

the interior of the water-soluble capsule-like complex, and they are flexible enough to breathe in such a way to allow guests to enter that are larger than the physical aperture.[169]

The organization of matter across length scales, starting from well-defined building blocks, is a key challenge in the design of advanced functional materials and devices. In this respect, we recently reported the spontaneous and controllable formation of micrometer-scale polyoxometalate tubes from crystals of a POM upon immersion in an aqueous solution containing a low concentration of an organic cation (Figure 27).[170] A membrane immediately forms around the crystal that then gives rise to micrometer-scale tubes; these tubes grow with vast aspect ratios at controllable rates along the surface on which the crystal is placed. The tubes consist of

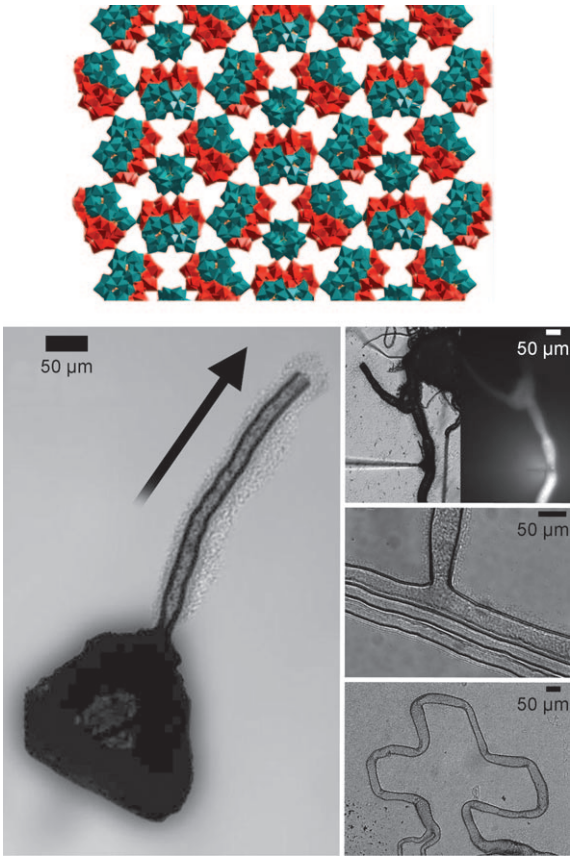

Figure 27. Growth of POM tubes. Top: Crystal structure of the polyoxometalate network formed from 3-connected (green) and 4-connected Keggin units (red). Bottom: Growth of the tube from the crystal over the period of 20 seconds (left), along with the ability to inject fluid into the tube without leakage (top right), the ability to join to tubes together (center right), and the ability to draw the tubes into predefined shapes (lower right).

an amorphous mixture of polyoxometalate-based anions and organic cations. It is possible to flow liquid through the tubes, and to control the direction of growth and overall tube diameter. We have demonstrated that the tube growth is driven by osmotic pressure within the membrane around the crystal, which then ruptures to release the pressure. These robust, self-growing, micrometer-scale tubes offer opportunities in many areas, including the growth of microfluidic devices and self-assembly of metal oxide based semi-permeable membranes for many diverse applications.

These tubes can be formed by almost any polyoxometalate precursor, depending on solubility control, thus opening up the possibility of fabricating micrometer-scale POM tubes with a material that is itself functional (exploiting the intrinsic function of the POM, such as catalysis, electrochemistry, or guest binding). We are attempting to fabricate catalytic tube structures using catalytically active POMs: the tetraruthe-

 © 2010 Wiley-VCH Verlag GmbH & Co. KGaA, Weinheim

nium POM[132,133] $[\{Ru_4O_4(OH)_2(H_2O)_4\}(\gamma\text{-}SiW_{10}O_{36})_2]^{10-}$ is being used to examine if water splitting can be accomplished within the tubes, and whether the tube material can be used as a membrane for gas–solvent separation. The growth of the POM tubes on ITO electrodes in a directional manner (to maximize packaging of the material) using a POM that can split water would be a very good example of a system that exploits several functions to achieve an aim.[170]

Finally, it is worth commenting that the polyoxometalates could help define the new field of inorganic complex synthetic systems/inorganic systems chemistry. This area involves the investigation of complex self-assembling and organizing systems that have emergent self-organizing properties, especially if systems can be pushed far from equilibrium into a high entropy-generating state.[171] The principles for supramolecular self-assembly, when applied to systems that can form dissipative structures, can lead to the emergence of adaptive chemistries and functional (nano)systems. The assembly of tubular microscale structures based upon polyoxometalate building blocks demonstrates this potential.[172] Combining synthetically adaptive chemistry with nanoscale to micrometer-scale structures may allow a totally new way of arranging and developing functional systems that could in the broadest sense show how inorganic chemistry really could come to life.

We would like to thank the EPSRC, the University of Glasgow and WestCHEM for funding, and Johannes Thiel for advice.

Received: May 11, 2009
Published online: February 3, 2010

[1] a) M. T. Pope, A. Müller, *Angew. Chem.* **1991**, *103*, 56 – 70; *Angew. Chem. Int. Ed. Engl.* **1991**, *30*, 34 – 48; b) A. Müller, S. Roy in *The Chemistry of Nanomaterials: Synthesis, Properties and Applications* (Hrsg.: C. N. R. Rao, A. Müller, A. K. Cheetham), Wiley-VCH, Weinheim, **2004**.
[2] C. L. Hill, *Chem. Rev.* **1998**, *98*, 1 – 2.
[3] D.-L. Long, E. Burkholder, L. Cronin, *Chem. Soc. Rev.* **2007**, *36*, 105 – 121.
[4] B. Hasenknopf, *Front. Biosci.* **2005**, *10*, 275 – 287.
[5] *Inorganic Synthesis*, Vol. 27, (Ed.: A. P. Ginsberg), **1990**, pp. 71 – 135.
[6] X. Fang, T. M. Anderson, C. L. Hill, *Angew. Chem.* **2005**, *117*, 3606 – 3610; *Angew. Chem. Int. Ed.* **2005**, *44*, 3540 – 3544.
[7] B. S. Bassil, M. H. Dickman, I. Römer, B. Kammer, U. Kortz, *Angew. Chem.* **2007**, *119*, 6305 – 6308; *Angew. Chem. Int. Ed.* **2007**, *46*, 6192 – 6195.
[8] D.-L. Long, D. Orr, G. Seeber, P. Kögerler, L. J. Farrugia, L. Cronin, *J. Clust. Sci.* **2003**, *14*, 313 – 315.
[9] "High Nuclearity Clusters: Iso and Heteropolyoxoanions and Relatives": L. Cronin, *Comprehensive Coordination Chemistry II*, *Vol. 7* (Eds.: J. A. McCleverty, T. J. Meyer), Elsevier, Amsterdam, **2004**, pp. 1 – 56.
[10] D.-L. Long, P. Kögerler, L. J. Farrugia, L. Cronin, *Angew. Chem.* **2003**, *115*, 4312 – 4315; *Angew. Chem. Int. Ed.* **2003**, *42*, 4180 – 4183.
[11] D.-L. Long, L. Cronin, *Chem. Eur. J.* **2006**, *12*, 3698 – 3706.
[12] A. Müller, E. Krickemeyer, J. Meyer, H. Bögge, F. Peters, W. Plass, E. Diemann, S. Dillinger, F. Nonnenbruch, M. Randerath, C. Menke, *Angew. Chem.* **1995**, *107*, 2293 – 2295; *Angew. Chem. Int. Ed. Engl.* **1995**, *34*, 2122 – 2126.
[13] A. Müller, E. Krickemeyer, H. Bögge, M. Schimidtmann, F. Peters, *Angew. Chem.* **1998**, *110*, 3567 – 3571; *Angew. Chem. Int. Ed.* **1998**, *37*, 3359 – 3363.
[14] C. Ritchie, E. Burkholder, P. Kögerler, L. Cronin, *Dalton Trans.* **2006**, 1712 – 1714.
[15] C. Ritchie, C. Streb, J. Thiel, S. G. Mitchell, H. N. Miras, D.-L. Long, T. Boyd, R. D. Peacock, T. McGlone, L. Cronin, *Angew. Chem.* **2008**, *120*, 6987 – 6990; *Angew. Chem. Int. Ed.* **2008**, *47*, 6881 – 6884.
[16] C. Fleming, D.-L. Long, N. McMillan, J. Johnston, N. Bovet, V. Dhanak, N. Gadegaard, P. Kögerler, L. Cronin, M. Kadodwala, *Nat. Nanotechnol.* **2008**, *3*, 229 – 233.
[17] S. Himeno, T. Katsuta, M. Takamoto, M. Hashimoto, *Bull. Chem. Soc. Jpn.* **2006**, *79*, 100 – 105.
[18] C. Y. Sun, S. X. Liu, D. D. Liang, K. Z. Shao, Y. H. Ren, Z. M. Su, *J. Am. Chem. Soc.* **2009**, *131*, 1883 – 1888.
[19] N. Zou, W. L. Chen, Y. G. Li, W. L. Liu, E. B. Wang, *Inorg. Chem. Commun.* **2008**, *11*, 1367 – 1370.
[20] C. Baffert, J. F. Boas, A. M. Bond, P. Kögerler, D.-L. Long, J. R. Pilbrow, L. Cronin, *Chem. Eur. J.* **2006**, *12*, 8472 – 8483.
[21] N. Fay, A. M. Bond, C. Baffert, J. F. Boas, J. R. Pilbrow, D.-L. Long, L. Cronin, *Inorg. Chem.* **2007**, *46*, 3502 – 3510.
[22] A. M. Douvas, E. Makarona, N. Glezos, P. Argitis, J. A. Mielczarski, and E. Mielczarski, *ACS Nano* **2008**, *2*, 733 – 742.
[23] D.-L. Long, Y. F. Song, E. F. Wilson, P. Kögerler, S. X. Guo, A. M. Bond, J. S. J. Hargreaves, L. Cronin, *Angew. Chem.* **2008**, *120*, 4456 – 4459; *Angew. Chem. Int. Ed.* **2008**, *47*, 4384 – 4387.
[24] D.-L. Long, P. Kögerler, A. D. C. Parenty, J. Fielden, L. Cronin, *Angew. Chem.* **2006**, *118*, 4916 – 4921; *Angew. Chem. Int. Ed.* **2006**, *45*, 4798 – 4803.
[25] J. Yan, D.-L. Long, E. F. Wilson, L. Cronin, *Angew. Chem.* **2009**, *121*, 4440 – 4444; *Angew. Chem. Int. Ed.* **2009**, *48*, 4376 – 4380.
[26] a) M. Sadakane, K. Yamagata, K. Kodato, K. Endo, K. Toriumi, Y. Ozawa, T. Ozeki, T. Nagai, Y. Matsui, N. Sakaguchi, W. D. Pyrz, D. J. Buttrey, D. A. Blom, T. Vogt, W. Ueda, *Angew. Chem.* **2009**, *121*, 3840 – 3844; *Angew. Chem. Int. Ed.* **2009**, *48*, 3782 – 3786; b) A. M. Todea, A. Merca, H. Bögge, T. Glaser, J. M. Pigga, M. L. K. Langston, T. Liu, R. Prozorov, M. Luban, C. Schröder, W. H. Casey, A. Müller, *Angew. Chem.* **2010**, *122*, 524 – 529; *Angew. Chem. Int. Ed.* **2010**, *49*, 514 – 519.
[27] a) C. Schäffer, A. Merca, H. Bögge, A. M. Todea, M. L. Kistler, T. B. Liu, R. Thouvenot, P. Gouzerh, A. Müller, *Angew. Chem.* **2009**, *121*, 155 – 159; *Angew. Chem. Int. Ed.* **2009**, *48*, 149 – 153; b) N. Leclerc-Laronze, J. Marrot, R. Thouvenot, E. Cadot, *Angew. Chem.* **2009**, *121*, 5086 – 5089; *Angew. Chem. Int. Ed.* **2009**, *48*, 4986 – 4989.
[28] G. E. Sigmon, D. K. Unruh, J. Ling, B. Weaver, M. Ward, L. Presprich, A. Simonetti, P. C. Burns, *Angew. Chem.* **2009**, *121*, 2775 – 2778; *Angew. Chem. Int. Ed.* **2009**, *48*, 2737 – 2740.
[29] *Polyoxometalate Molecular Science* (Eds.: J. J. Borrás-Almenar, E. Coronado, A. Müller, M. T. Pope), Kluwer, Dordrecht, **2003**.
[30] R. P. Bontchev, M. Nyman, *Angew. Chem.* **2006**, *118*, 6822 – 6824; *Angew. Chem. Int. Ed.* **2006**, *45*, 6670 – 6672.
[31] J. Y. Niu, P. T. Ma, H. Y. Niu, J. Li, J. W. Zhao, Y. Song, J. P. Wang, *Chem. Eur. J.* **2007**, *13*, 8739 – 8748.
[32] R. Tsunashima, D.-L. Long, H. N. Miras, D. Gabb, C. P. Pradeep, L. Cronin, *Angew. Chem.* **2010**, *122*, 117 – 120; *Angew. Chem. Int. Ed.* **2010**, *49*, 113 – 116.
[33] C. A. Ohlin, E. M. Villa, J. C. Fettinger, W. H. Casey, *Angew. Chem.* **2008**, *120*, 5716 – 5718; *Angew. Chem. Int. Ed.* **2008**, *47*, 5634 – 5636.
[34] E. V. Chubarova, M. H. Dickman, B. Keita, L. Nadjo, F. Miserque, M. Mifsud, I. W. C. E. Arends, U. Kortz, *Angew. Chem.* **2008**, *120*, 9685 – 9689; *Angew. Chem. Int. Ed.* **2008**, *47*, 9542 – 9546.
[35] M. Pley, M. S. Wickleder, *Angew. Chem.* **2004**, *116*, 4262 – 4264; *Angew. Chem. Int. Ed.* **2004**, *43*, 4168 – 4170.

 © 2010 Wiley-VCH Verlag GmbH & Co. KGaA, Weinheim

[36] C. L. Hill, *Nature* **2008**, *455*, 1045.
[37] T. M. Anderson, W. A. Neiwert, M. L. Kirk, P. M. B. Piccoli, A. J. Schultz, T. F. Koetzle, D. G. Musaev, K. Morokuma, R. Cao, C. L. Hill, *Science* **2004**, *306*, 2074 – 2077.
[38] T. M. Anderson, R. Cao, E. Slonkina, B. Hedman, K. O. Hodgson, K. I. Hardcastle, W. A. Neiwert, S. X. Wu, M. L. Kirk, S. Knottenbelt, E. C. Depperman, B. Keita, L. Nadjo, D. G. Musaev, K. Morokuma, C. L. Hill, *J. Am. Chem. Soc.* **2005**, *127*, 11948 – 11949.
[39] R. Cao, T. M. Anderson, P. M. B. Piccoli, A. J. Schultz, T. F. Koetzle, Y. V. Geletii, E. Slonkina, B. Hedman, K. O. Hodgson, K. I. Hardcastle, X. Fang, M. L. Kirk, S. Knottenbelt, P. Kögerler, D. G. Musaev, K. Morokuma, M. Takahashi, C. L. Hill, *J. Am. Chem. Soc.* **2007**, *129*, 11118 – 11133.
[40] a) R. Cao, T. M. Anderson, D. A. Hillesheim, P. Kögerler, K. I. Hardcastle, C. L. Hill, *Angew. Chem.* **2008**, *120*, 9520 – 9522; *Angew. Chem. Int. Ed.* **2008**, *47*, 9380 – 9382; b) U. Kortz, U. Lee, H.-C. Joo, K.-M. Park, S. S. Mal, M. H. Dickman, G. B. Jameson, *Angew. Chem.* **2008**, *120*, 9523 – 9524; *Angew. Chem. Int. Ed.* **2008**, *47*, 9383 – 9384.
[41] E. Poverenov, I. Efremenko, A. I. Frenkel, Y. Ben-David, L. J. W. Shimon, G. Leitus, L. Konstantinovski, J. M. L. Martin, D. Milstein, *Nature* **2008**, *455*, 1093 – 1096.
[42] D. Barats, G. Leitus, R. Popovitz-Biro, L. J. W. Shimon, R. Neumann, *Angew. Chem.* **2008**, *120*, 10056 – 10060; *Angew. Chem. Int. Ed.* **2008**, *47*, 9908 – 9912.
[43] B. S. Bassil, S. S. Mal, M. H. Dickman, U. Kortz, H. Oelrich, L. Walder, *J. Am. Chem. Soc.* **2008**, *130*, 6696 – 6697.
[44] L. K. Yan, X. López, J. J. Carbó, R. Sniatynsky, D. C. Duncan, J. M. Poblet, *J. Am. Chem. Soc.* **2008**, *130*, 8223 – 8233.
[45] B. Hasenknopf, K. Micoine, E. Lacôte, S. Thorimbert, M. Malacria, R. Thouvenot, *Eur. J. Inorg. Chem.* **2008**, 5001 – 5013.
[46] Y. Q. Lan, S. L. Li, Z. M. Su, K. Z. Shao, J. F. Ma, X. L. Wang, E. B. Wang, *Chem. Commun.* **2008**, 58 – 60.
[47] C. Streb, D.-L. Long, L. Cronin, *Chem. Commun.* **2007**, 471 – 473.
[48] H. Y. An, E. B. Wang, D. R. Xiao, Y. G. Li, Z. M. Su, L. Xu, *Angew. Chem.* **2006**, *118*, 918 – 922; *Angew. Chem. Int. Ed.* **2006**, *45*, 904 – 908.
[49] Y. Q. Lan, S. L. Li, X. L. Wang, K. Z. Shao, D. Y. Du, Z. M. Su, E. B. Wang, *Chem. Eur. J.* **2008**, *14*, 9999 – 10006.
[50] D.-L. Long, P. Kögerler, L. J. Farrugia, L. Cronin, *Chem. Asian J.* **2006**, *1*, 352 – 357.
[51] H. N. Miras, E. F. Wilson, L. Cronin, *Chem. Commun.* **2009**, 1297 – 1311.
[52] D.-L. Long, C. Streb, Y. F. Song, S. Mitchell, L. Cronin, *J. Am. Chem. Soc.* **2008**, *130*, 1830 – 1832, and references therein.
[53] H. N. Miras, D.-L. Long, P. Kögerler, L. Cronin, *Dalton Trans.* **2008**, 214 – 221.
[54] H. N. Miras, J. Yan, D.-L. Long, L. Cronin, *Angew. Chem.* **2008**, *120*, 8548 – 8551; *Angew. Chem. Int. Ed.* **2008**, *47*, 8420 – 8423.
[55] C. P. Pradeep, D.-L. Long, G. N. Newton, Y. F. Song, L. Cronin, *Angew. Chem.* **2008**, *120*, 4460 – 4463; *Angew. Chem. Int. Ed.* **2008**, *47*, 4388 – 4391.
[56] E. F. Wilson, H. Abbas, B. J. Duncombe, C. Streb, D.-L. Long, L. Cronin, *J. Am. Chem. Soc.* **2008**, *130*, 13876 – 13884.
[57] Y. F. Song, D.-L. Long, S. E. Kelly, L. Cronin, *Inorg. Chem.* **2008**, *47*, 9137 – 9139.
[58] M. T. Ma, T. Waters, K. Beyer, R. Palamarczuk, P. J. S. Richardt, R. A. J. O'Hair, A. G. Wedd, *Inorg. Chem.* **2009**, *48*, 598 – 606.
[59] C. A. Ohlin, E. M. Villa, J. C. Fettinger, W. H. Casey, *Angew. Chem.* **2008**, *120*, 8375 – 8378; *Angew. Chem. Int. Ed.* **2008**, *47*, 8251 – 8254.
[60] T. B. Liu, E. Diemann, H. L. Li, A. W. M. Dress, A. Müller, *Nature* **2003**, *426*, 59 – 62.
[61] G. Liu, T. B. Liu, *Langmuir* **2005**, *21*, 2713 – 2720.
[62] A. Proust, R. Thouvenot, P. Gouzerh, *Chem. Commun.* **2008**, 1837 – 1852.
[63] Z. H. Peng, *Angew. Chem.* **2004**, *116*, 948 – 953; *Angew. Chem. Int. Ed.* **2004**, *43*, 930 – 935.
[64] J. Hao, Y. Xia, L. S. Wang, L. Ruhlmann, Y. L. Zhu, Q. Li, P. C. Yin, Y. G. Wei, H. Y. Guo, *Angew. Chem.* **2008**, *120*, 2666 – 2670; *Angew. Chem. Int. Ed.* **2008**, *47*, 2626 – 2630.
[65] Y. L. Zhu, L. S. Wang, J. Hao, P. C. Yin, J. Zhang, Q. Li, L. Zhu, Y. G. Wei, *Chem. Eur. J.* **2009**, *15*, 3076 – 3080.
[66] Y. F. Song, D.-L. Long, L. Cronin, *Angew. Chem.* **2007**, *119*, 3974 – 3978; *Angew. Chem. Int. Ed.* **2007**, *46*, 3900 – 3904.
[67] Y. F. Song, N. McMillan, D.-L. Long, J. Thiel, Y. L. Ding, H. S. Chen, N. Gadegaard, L. Cronin, *Chem. Eur. J.* **2008**, *14*, 2349 – 2354.
[68] J. Li, I. Huth, L. M. Chamoreau, B. Hasenknopf, E. Lacôte, S. Thorimbert, M. Malacria, *Angew. Chem.* **2009**, *121*, 2069 – 2072; *Angew. Chem. Int. Ed.* **2009**, *48*, 2035 – 2038.
[69] F. Odobel, M. Séverac, Y. Pellegrin, E. Blart, C. Fosse, C. Cannizzo, C. R. Mayer, K. J. Elliott, A. Harriman, *Chem. Eur. J.* **2009**, *15*, 3130 – 3138.
[70] L. F. Piedra-Garza, M. H. Dickman, O. Moldovan, H. J. Breunig, U. Kortz, *Inorg. Chem.* **2009**, *48*, 411 – 413.
[71] D.-L. Long, H. Abbas, P. Kögerler, L. Cronin, *J. Am. Chem. Soc.* **2004**, *126*, 13880 – 13881.
[72] D.-L. Long, O. Brucher, C. Streb, L. Cronin, *Dalton Trans.* **2006**, 2852 – 2860.
[73] A. H. Ismail, M. H. Dickman, U. Kortz, *Inorg. Chem.* **2009**, *48*, 1559 – 1565.
[74] C. P. Pradeep, D.-L. Long, P. Kögerler, L. Cronin, *Chem. Commun.* **2007**, 4254 – 4256.
[75] a) X. K. Fang, P. Kögerler, *Angew. Chem.* **2008**, *120*, 8243 – 8246; *Angew. Chem. Int. Ed.* **2008**, *47*, 8123 – 8126; b) X. K. Fang, P. Kögerler, *Chem. Commun.* **2008**, 3396 – 3398.
[76] F. Hussain, R. W. Gable, M. Speldrich, P. Kögerler, C. Boskovic, *Chem. Commun.* **2009**, 328 – 330.
[77] M. N. Sokolov, V. S. Korenev, N. V. Izarova, E. V. Peresypkina, C. Vicent, V. P. Fedin, *Inorg. Chem.* **2009**, *48*, 1805 – 1807.
[78] S. S. Mal, M. H. Dickman, U. Kortz, *Chem. Eur. J.* **2008**, *14*, 9851 – 9855.
[79] C. P. Pradeep, D.-L. Long, C. Streb, L. Cronin, *J. Am. Chem. Soc.* **2008**, *130*, 14946 – 14947.
[80] M. Ibrahim, M. H. Dickman, A. Suchopar, U. Kortz, *Inorg. Chem.* **2009**, *48*, 1649 – 1654.
[81] S. Uchida, R. Kawamoto, N. Mizuno, *Inorg. Chem.* **2006**, *45*, 5136 – 5144.
[82] T. Akutagawa, D. Endo, F. Kudo, S. I. Noro, S. Takeda, L. Cronin, T. Nakamura, *Cryst. Growth Des.* **2008**, *8*, 812 – 816.
[83] J. L. Xie, B. F. Abrahams, A. G. Wedd, *Chem. Commun.* **2008**, 576 – 578.
[84] E. Coronado, C. Giménez-Saiz, C. Martí-Gastaldo, *Eng. Cryst. Mater. Proper.* **2008**, 173 – 191.
[85] H. Abbas, C. Streb, A. L. Pickering, A. R. Neil, D.-L. Long, L. Cronin, *Cryst. Growth Des.* **2008**, *8*, 635 – 642.
[86] Y. F. Song, H. Abbas, C. Ritchie, N. McMillian, D.-L. Long, N. Gadegaard, L. Cronin, *J. Mater. Chem.* **2007**, *17*, 1903 – 1908.
[87] C. Streb, C. Ritchie, D.-L. Long, P. Kögerler, L. Cronin, *Angew. Chem.* **2007**, *119*, 7723 – 7726; *Angew. Chem. Int. Ed.* **2007**, *46*, 7579 – 7582.
[88] T. Arumuganathan, S. K. Das, *Inorg. Chem.* **2009**, *48*, 496 – 507.
[89] J. Thiel, C. Ritchie, C. Streb, D.-L. Long, L. Cronin, *J. Am. Chem. Soc.* **2009**, *131*, 4180 – 4181.
[90] A. X. Tian, J. Ying, J. Peng, J. Q. Sha, H. J. Pang, P. P. Zhang, Y. Chen, M. Zhu, Z. M. Su, *Cryst. Growth Des.* **2008**, *8*, 3717 – 3724.
[91] M. Jiang, T. F. Jiao, M. H. Liu, *New J. Chem.* **2008**, *32*, 959 – 965.
[92] M. Xu, Y. C. Li, W. Li, C. Q. Sun, L. X. Wu, *J. Colloid Interface Sci.* **2007**, *315*, 753 – 760.

 © 2010 Wiley-VCH Verlag GmbH & Co. KGaA, Weinheim

[93] T. Ito, H. Yashiro, T. Yamase, *Langmuir* **2006**, *22*, 2806 – 2810.
[94] T. Akutagawa, R. Jin, R. Tunashima, S. Noro, L. Cronin, T. Nakamura, *Langmuir* **2008**, *24*, 231 – 238.
[95] S. Y. Gao, R. Cao, C. P. Yang, *J. Colloid Interface Sci.* **2008**, *324*, 156 – 166.
[96] D. G. Kurth, *Sci. Technol. Adv. Mater.* **2008**, *9*, 014103.
[97] S. Q. Liu, H. Mohwald, D. Volkmer, D. G. Kurth, *Langmuir* **2006**, *22*, 1949 – 1951.
[98] Y. Nagaoka, S. Shiratori, Y. Einaga, *Chem. Mater.* **2008**, *20*, 4004 – 4010.
[99] G. Bazzan, W. Smith, L. C. Francesconi, C. M. Drain, *Langmuir* **2008**, *24*, 3244 – 3249.
[100] Y. F. Song, N. McMillan, D.-L. Long, S. Kane, J. Malm, M. O. Riehle, C. P. Pradeep, N. Gadegaard, L. Cronin, *J. Am. Chem. Soc.* **2009**, *131*, 1340 – 1341.
[101] L. Cronin, *Angew. Chem.* **2006**, *118*, 3656 – 3658; *Angew. Chem. Int. Ed.* **2006**, *45*, 3576 – 3578.
[102] J. Zhang, Y. F. Song, L. Cronin, T. B. Liu, *J. Am. Chem. Soc.* **2008**, *130*, 14408 – 14409.
[103] H. L. Li, H. Sun, W. Qi, M. Xu, L. X. Wu, *Angew. Chem.* **2007**, *119*, 1322 – 1325; *Angew. Chem. Int. Ed.* **2007**, *46*, 1300 – 1303.
[104] B. L. Chen, H. J. Jiang, Y. Zhu, A. Cammers, J. P. Selegue, *J. Am. Chem. Soc.* **2005**, *127*, 4166 – 4167.
[105] G. Liu, T. B. Liu, S. S. Mal, U. Kortz, *J. Am. Chem. Soc.* **2006**, *128*, 10103 – 10110.
[106] P. P. Mishra, J. Pigga, T. B. Liu, *J. Am. Chem. Soc.* **2008**, *130*, 1548 – 1549.
[107] P. P. Mishra, J. Jing, L. C. Francesconi, T. B. Liu, *Langmuir* **2008**, *24*, 9308 – 9313.
[108] A. A. Verhoeff, M. L. Kistler, A. Bhatt, J. Pigga, J. Groenewold, M. Klokkenburg, S. Veen, S. Roy, T. B. Liu, W. K. Kegel, *Phys. Rev. Lett.* **2007**, *99*, 066104.
[109] G. Maayan, R. Popovitz-Biro, R. Neumann, *J. Am. Chem. Soc.* **2006**, *128*, 4968 – 4969.
[110] J. Zhang, B. Keita, L. Nadjo, I. M. Mbomekalle, T. B. Liu, *Langmuir* **2008**, *24*, 5277 – 5283.
[111] R. Y. Wang, D. Z. Jia, L. Zhang, L. Liu, Z. P. Guo, B. Q. Li, J. X. Wang, *Adv. Funct. Mater.* **2006**, *16*, 687 – 692.
[112] M. Boujtita, J. Boixel, E. Blart, C. R. Mayer, F. Odobel, *Polyhedron* **2008**, *27*, 688 – 692.
[113] J. A. Fernández, X. López, C. Bo, C. de Graaf, E. J. Baerends, J. M. Poblet, *J. Am. Chem. Soc.* **2007**, *129*, 12244 – 12253.
[114] B. Keita, T. B. Liu, L. Nadjo, *J. Mater. Chem.* **2009**, *19*, 19 – 33.
[115] W. Qi, H. L. Li, L. X. Wu, *J. Phys. Chem. B* **2008**, *112*, 8257 – 8263.
[116] Z. Kang, Y. Liu, C. H. A. Tsang, D. D. D. Ma, E. B. Wang, S. T. Lee, *Chem. Commun.* **2009**, 413 – 415.
[117] W. Guan, G. C. Yang, C. G. Liu, P. Song, L. Fang, L. K. Yan, Z. M. Su, *Inorg. Chem.* **2008**, *47*, 5245 – 5252.
[118] J. Lehmann, A. Gaita-Ariño, E. Coronado, D. Loss, *Nat. Nanotechnol.* **2007**, *2*, 312 – 317.
[119] C. J. Calzado, J. M. Clemente-Juan, E. Coronado, A. Gaita-Arinõ, N. Suaud, *Inorg. Chem.* **2008**, *47*, 5889 – 5901.
[120] C. Aronica, G. Chastanet, E. Zueva, S. A. Borshch, J. M. Clemente-Juan, D. Luneau, *J. Am. Chem. Soc.* **2008**, *130*, 2365 – 2371.
[121] P. Mialane, C. Duboc, J. Marrot, E. Rivière, A. Dolbecq, F. Sécheresse, *Chem. Eur. J.* **2006**, *12*, 1950 – 1959.
[122] J. W. Zhao, J. Zhang, S. T. Zheng, G. Y. Yang, *Chem. Commun.* **2008**, 570 – 572.
[123] T. Yamase, H. Abe, E. Ishikawa, H. Nojiri, Y. Ohshima, *Inorg. Chem.* **2009**, *48*, 138 – 148.
[124] B. Botar, P. Kögerler, *Dalton Trans.* **2008**, 3150 – 3152.
[125] Q. Wu, Y. G. Li, Y. H. Wang, E. B. Wang, Z. M. Zhang, R. Clerac, *Inorg. Chem.* **2009**, *48*, 1606 – 1612.
[126] C. Ritchie, A. Ferguson, H. Nojiri, H. N. Miras, Y. F. Song, D.-L. Long, E. Burkholder, M. Murrie, P. Kögerler, E. K. Brechin, L. Cronin, *Angew. Chem.* **2008**, *120*, 5691 – 5694; *Angew. Chem. Int. Ed.* **2008**, *47*, 5609 – 5612.
[127] M. A. AlDamen, J. M. Clemente-Juan, E. Coronado, C. Marti-Gastaldo, A. Gaita-Ariño, *J. Am. Chem. Soc.* **2008**, *130*, 8874 – 8875.
[128] N. Mizuno, K. Yamaguchi, *Chem. Rec.* **2006**, *6*, 12 – 22.
[129] J. Piera, J. E. Bäckvall, *Angew. Chem.* **2008**, *120*, 3558 – 3576; *Angew. Chem. Int. Ed.* **2008**, *47*, 3506 – 3523.
[130] C. L. Hill, *J. Mol. Catal. A* **2007**, *262*, 2 – 6.
[131] M. Carraro, A. Sartorel, G. Scorrano, T. Carofiglio, M. Bonchio, *Synthesis* **2008**, 1971 – 1978.
[132] A. Sartorel, M. Carraro, G. Scorrano, R. De Zorzi, S. Geremia, N. D. McDaniel, S. Bernhard, M. Bonchio, *J. Am. Chem. Soc.* **2008**, *130*, 5006 – 5007.
[133] Y. V. Geletii, B. Botar, P. Kögerler, D. A. Hillesheim, D. G. Musaev, C. L. Hill, *Angew. Chem.* **2008**, *120*, 3960 – 3963; *Angew. Chem. Int. Ed.* **2008**, *47*, 3896 – 3899.
[134] N. V. Maksimchuk, M. N. Timofeeva, M. S. Melgunov, A. N. Shmakov, Y. A. Chesalov, D. N. Dybtsev, V. P. Fedin, O. A. Kholdeeva, *J. Catal.* **2008**, *257*, 315 – 323.
[135] A. M. Al-Ajlouni, O. Sağlam, T. Diafla, F. E. Kühn, *J. Mol. Catal. A* **2008**, *287*, 159 – 164.
[136] L. L. Liu, C. C. Chen, X. F. Hu, T. Mohamood, W. H. Ma, J. Lin, J. C. Zhao, *New J. Chem.* **2008**, *32*, 283 – 289.
[137] R. H. Ingle, A. Vinu, S. B. Halligudi, *Catal. Commun.* **2008**, *9*, 931 – 938.
[138] C. Galli, P. Gentili, A. S. N. Pontes, J. A. F. Gamelas, D. V. Evtuguin, *New J. Chem.* **2007**, *31*, 1461 – 1467.
[139] G. Maayan, R. Neumann, *Catal. Lett.* **2008**, *123*, 41 – 45.
[140] D. W. Pan, J. H. Chen, W. Y. Tao, L. H. Nie, S. Z. Yao, *Langmuir* **2006**, *22*, 5872 – 5876.
[141] E. Cartuyvels, G. Absillis, T. N. Parac-Vogt, *Chem. Commun.* **2008**, 85 – 87.
[142] G. Absillis, E. Cartuyvels, R. Van Deun, T. N. Parac-Vogt, *J. Am. Chem. Soc.* **2008**, *130*, 17400 – 17408.
[143] A. Alhanash, E. F. Kozhevnikova, I. V. Kozhevnikov, *Catal. Lett.* **2008**, *120*, 307 – 311.
[144] H. Hori, A. Yamamoto, K. Koike, S. Kutsuna, M. Murayama, A. Yoshimoto, R. Arakawa, *Appl. Catal. B* **2008**, *82*, 58 – 66.
[145] K. Kamata, S. Yamaguchi, M. Kotani, K. Yamaguchi, N. Mizuno, *Angew. Chem.* **2008**, *120*, 2441 – 2444; *Angew. Chem. Int. Ed.* **2008**, *47*, 2407 – 2410.
[146] Y. Kikukawa, S. Yamaguchi, K. Tsuchida, Y. Nakagawa, K. Uehara, K. Yamaguchi, N. Mizuno, *J. Am. Chem. Soc.* **2008**, *130*, 5472 – 5478.
[147] V. Mirkhani, M. Moghadam, S. Tangestaninejad, I. Mohammadpoor-Baltork, N. Rasouli, *Catal. Commun.* **2008**, *9*, 2171 – 2174.
[148] J. Ettedgui, R. Neumann, *J. Am. Chem. Soc.* **2009**, *131*, 4 – 5.
[149] J. Macht, M. J. Janik, M. Neurock, E. Iglesia, *J. Am. Chem. Soc.* **2008**, *130*, 10369 – 10379.
[150] K. Inumaru, T. Ishihara, Y. Kamiya, T. Okuhara, S. Yamanaka, *Angew. Chem.* **2007**, *119*, 7769 – 7772; *Angew. Chem. Int. Ed.* **2007**, *46*, 7625 – 7628.
[151] Y. Kikukawa, S. Yamaguchi, Y. Nakagawa, K. Uehara, S. Uchida, K. Yamaguchi, N. Mizuno, *J. Am. Chem. Soc.* **2008**, *130*, 15872 – 15878.
[152] Y. B. Xie, *Adv. Funct. Mater.* **2006**, *16*, 1823 – 1831.
[153] A. V. Sankarraj, S. Ramakrishnan, C. Shannon, *Langmuir* **2008**, *24*, 632 – 634.
[154] W. B. Kim, T. Voitl, G. J. Rodriguez-Rivera, J. A. Dumesic, *Science* **2004**, *305*, 1280 – 1283.
[155] A. Ogata, H. Yanagie, E. Ishikawa, Y. Morishita, S. Mitsui, A. Yamashita, K. Hasumi, S. Takamoto, T. Yamase, M. Eriguchi, *Br. J. Cancer* **2008**, *98*, 399 – 409.
[156] H. Yanagie, A. Ogata, S. Mitsui, T. Hisa, T. Yamase, M. Eriguchi, *Biomed. Pharmacother.* **2006**, *60*, 349 – 352.

© 2010 Wiley-VCH Verlag GmbH & Co. KGaA, Weinheim

[157] S. Mitsui, A. Ogata, H. Yanagie, H. Kasano, T. Hisa, T. Yamase, M. Eriguchi, *Biomed. Pharmacother.* **2006**, *60*, 353 – 358.
[158] R. Prudent, V. Moucadel, B. Laudet, C. Barette, L. Lafanechère, B. Hasenknopf, J. Li, S. Bareyt, E. Lacôte, S. Thorimbert, M. Malacria, P. Gouzerh, C. Cochet, *Chem. Biol.* **2008**, *15*, 683 – 692.
[159] K. Dan, T. Yamase, *Biomed. Pharmacother.* **2006**, *60*, 169 – 173.
[160] S. Shigeta, S. Mori, T. Yamase, N. Yamamoto, N. Yamamoto, *Biomed. Pharmacother.* **2006**, *60*, 211 – 219.
[161] M. Inoue, T. Suzuki, Y. Fujita, M. Oda, N. Matsumoto, T. Yamase, *J. Inorg. Biochem.* **2006**, *100*, 1225 – 1233.
[162] E. Bae, J. W. Lee, B. H. Hwang, J. Yeo, J. Yoon, H. J. Cha, W. Choi, *Chemosphere* **2008**, *72*, 174 – 181.
[163] F. Carn, N. Steunou, M. Djabourov, T. Coradin, F. Ribot, J. Livage, *Soft Matter* **2008**, *4*, 735 – 738.
[164] M. Nyman, J. M. Bieker, S. G. Thoma, D. E. Trudell, *J. Colloid Interface Sci.* **2007**, *316*, 968 – 976.
[165] a) J. Schemberg, K. Schneider, D. Fenske, A. Müller, *ChemBioChem* **2008**, *9*, 595 – 602; b) J. Schemberg, K. Schneider, U. Demmer, E. Warkentin, A. Müller, U. Ermler, *Angew. Chem.* **2007**, *119*, 2460 – 2465; *Angew. Chem. Int. Ed.* **2007**, *46*, 2408 – 2413.
[166] G. Zhang, B. Keita, C. T. Craescu, S. Miron, P. de Oliveira, L. Nadjo, *J. Phys. Chem. B* **2007**, *111*, 11253 – 11259.
[167] H. Wille, M. Shanmugam, M. Murugesu, J. Ollesch, G. Stubbs, J. R. Long, J. G. Safar, S. B. Prusiner, *Proc. Natl. Acad. Sci. USA* **2009**, *106*, 3740 – 3745.
[168] J. Sloan, G. Matthewman, C. Dyer-Smith, A. Y. Sung, Z. Liu, K. Suenaga, A. I. Kirkland, E. Flahaut, *Acs Nano* **2008**, *2*, 966 – 976.
[169] a) A. Ziv, A. Grego, S. Kopilevich, L. Zeiri, P. Miro, C. Bo, A. Müller, I. A. Weinstock, *J. Am. Chem. Soc.* **2009**, *131*, 6380 – 6382; b) C. Schäffer, H. Bögge, A. Merca, I. A. Weinstock, D. Rehder, E. T. K. Haupt, A. Müller, *Angew. Chem.* **2009**, *121*, 8195 – 8200; *Angew. Chem. Int. Ed.* **2009**, *48*, 8051 – 8056; c) A. Müller, F. L. Sousa, A. Merca, H. Bögge, P. Miró, J. A. Fernández, J. M. Poblet, C. Bo, *Angew. Chem.* **2009**, *121*, 6048 – 6051; *Angew. Chem. Int. Ed.* **2009**, *48*, 5934 – 5937; d) Ref. [26b].
[170] a) C. Ritchie, G. J. T. Cooper, Y. Song, C. Streb, H. Yin, A. D. C. Parenty, D. A. MacLaren, L. Cronin, *Nat. Chem.* **2009**, *1*, 47 – 52; b) G. J. T. Cooper, L. Cronin, *J. Am. Chem. Soc.* **2009**, *131*, 8368 – 8369.
[171] H. N. Miras, G. J. T. Cooper, D.-L. Long, H. Bögge, A. Müller, C. Streb, L. Cronin, *Science* **2010**, *327*, 72 – 74.
[172] L. Cronin, N. Krasnogor, B. G. Davis, C. Alexander, N. Robertson, J. H. G. Steinke, S. L. M. Schroeder, A. N. Khlobystov, G. J. T. Cooper, P. M. Gardner, P. Siepmann, B. J. Whitaker, D. Marsh, *Nat. Biotechnol.* **2006**, *24*, 1203 – 1206.

 © 2010 Wiley-VCH Verlag GmbH & Co. KGaA, Weinheim